Geochemistry Geophysics Geosystems G3
AN ELECTRONIC JOURNAL OF THE EARTH SCIENCES
Published by AGU and the Geochemical Society

Article
Volume 7, Number 7
26 July 2006
Q07P15, doi:10.1029/2005GC001019
ISSN: 1525-2027

Assessing the effect of dissolution on planktonic foraminiferal Mg/Ca ratios: Evidence from Caribbean core tops

Marcus Regenberg and Dirk Nürnberg
Leibniz Institute of Marine Sciences IFM-GEOMAR, Wischhofstr. 1–3, D-24148 Kiel, Germany (mregenberg@ifm-geomar.de; dnuernberg@ifm-geomar.de)

Silke Steph
Leibniz Institute of Marine Sciences IFM-GEOMAR, Wischhofstr. 1–3, D-24148 Kiel, Germany

Now at Alfred Wegener Institute for Polar and Marine Research AWI, Am Alten Hafen 26, D-27568 Bremerhaven, Germany (ssteph@awi-bremerhaven.de)

Jeroen Groeneveld
Leibniz Institute of Marine Sciences IFM-GEOMAR, Wischhofstr. 1–3, D-24148 Kiel, Germany

Now at Research Center Ocean Margins RCOM, University of Bremen, Leobener Str., D-28359 Bremen, Germany (jgroeneveld@uni-bremen.de)

Dieter Garbe-Schönberg
Institute of Geosciences, University of Kiel, Ludewig-Meyn-Str. 10, D-24118 Kiel, Germany (dgs@gpi.uni-kiel.de)

Ralf Tiedemann
Leibniz Institute of Marine Sciences IFM-GEOMAR, Wischhofstr. 1–3, D-24148 Kiel, Germany

Now at Alfred Wegener Institute for Polar and Marine Research AWI, Am Alten Hafen 26, D-27568 Bremerhaven, Germany (rtiedemann@awi.bremerhaven.de)

Wolf-Christian Dullo
Leibniz Institute of Marine Sciences IFM-GEOMAR, Wischhofstr. 1–3, D-24148 Kiel, Germany (cdullo@ifm-geomar.de)

[1] In order to assess the dissolution effect on foraminiferal Mg/Ca ratios, we analyzed Mg/Ca of seven planktonic foraminiferal species and four of their varieties from Caribbean core tops from ~900–4700 m water depth. Depending on the foraminiferal species and variety, Mg/Ca start to decline linearly below $\Delta[CO_3^{2-}]$ levels of ~18–26 μmol/kg by ~0.04–0.11 mmol/mol per 1 μmol/kg $\Delta[CO_3^{2-}]$, similar to decreases of ~0.5–0.8 mmol/mol per kilometer below ~2500–3000 m water depth. Above these species-specific critical levels, Mg/Ca remains stable with higher intraspecific Mg/Ca variability than below. We developed routines to correct Mg/Ca from below these critical thresholds for dissolution effects, which

reduce the overall intraspecific variability by ~24–64%, and provide dissolution-corrected Mg/Ca appropriate to calculate Holocene paleotemperatures. When taking into account only dissolution-unaffected Mg/Ca from <2000 m, the systematic succession of foraminiferal species according to their Mg/Ca reflects expected calcification depths.

Components: 4970 words, 9 figures, 4 tables.

Keywords: carbonate ion concentration; dissolution effect; Mg/Ca paleothermometry; planktonic foraminifera.

Index Terms: 3344 Atmospheric Processes: Paleoclimatology (0473, 4900); 3030 Marine Geology and Geophysics: Micropaleontology (0459, 4944).

Received 14 May 2005; **Revised** 7 April 2006; **Accepted** 27 April 2006; **Published** 26 July 2006.

Regenberg, M., D. Nürnberg, S. Steph, J. Groeneveld, D. Garbe-Schönberg, R. Tiedemann, and W.-C. Dullo (2006), Assessing the effect of dissolution on planktonic foraminiferal Mg/Ca ratios: Evidence from Caribbean core tops, *Geochem. Geophys. Geosyst.*, *7*, Q07P15, doi:10.1029/2005GC001019.

Theme: Development of the Foraminiferal Mg/Ca Proxy for Paleoceanography
Guest Editor: Pamela Martin

1. Introduction

[2] Mg/Ca ratios of planktonic foraminiferal tests have been developed as a powerful tool in paleoceanography to assess past ocean temperatures [e.g., *Elderfield and Ganssen*, 2000; *Nürnberg*, 2000; *Lea*, 2003]. This proxy became widely used mainly due to the fact that both stable oxygen isotopes ($\delta^{18}O$) and Mg/Ca can be measured within the same biotic carrier, which ensures the recording of the same seasonality and/or habitat effects that may occur when proxy data from different faunal groups are compared. Most advantageous, combined measurements of Mg/Ca and $\delta^{18}O$ allow to extract the $\delta^{18}O$ record of past upper ocean water, and accordingly salinity variations [e.g., *Nürnberg*, 2000; *Lea*, 2003; *Schmidt et al.*, 2004; *Pahnke and Zahn*, 2005; *Nürnberg and Groeneveld*, 2006].

[3] The accurate assessment of paleotemperatures from different depth levels of the ocean is a prerequisite to reconstruct and model past changes in salinity and density gradients, stratification patterns, and thus thermohaline circulation. The exponential dependence of Mg/Ca ratios on temperature within single planktonic foraminiferal species is well-studied, resulting in a variety of species-specific [*Nürnberg*, 1995; *Nürnberg et al.*, 1996a, 1996b, 2000; *Lea et al.*, 1999, 2000; *Mashiotta et al.*, 1999; *Dekens et al.*, 2002; *Rosenthal and Lohmann*, 2002; *Whitko et al.*, 2002; *McKenna and Prell*, 2004; *McConnell and Thunell*, 2005] and multi-species calibration curves [*Elderfield and Ganssen*, 2000; *Anand et al.*, 2003]. The accuracy of the Mg/Ca paleothermometry is specified with ±0.2–1.2°C [*Nürnberg*, 1995; *Nürnberg et al.*, 1996a, 2000; *Hastings et al.*, 1998; *Elderfield and Ganssen*, 2000; *Lea et al.*, 2000; *Dekens et al.*, 2002; *Anand et al.*, 2003]. Nevertheless, the influence of factors on Mg/Ca other than temperature, which may affect the amount of magnesium incorporated into foraminiferal tests during calcification, is still debated. Primary effects such as intraspecies and ontogenetic variations [e.g., *Nürnberg et al.*, 1996a], pH, carbonate ion concentration ($[CO_3^{2-}]$), and salinity [e.g., *Nürnberg et al.*, 1996a, 1996b; *Lea et al.*, 1999; *Russell et al.*, 2004] as well as secondary (diagenetic) effects such as preferential removal of Mg^{2+} during calcite dissolution [e.g., *Savin and Douglas*, 1973; *Cronblad and Malmgren*, 1981; *Brown and Elderfield*, 1996; *Rosenthal et al.*, 2000; *Rosenthal and Lohmann*, 2002; *Dekens et al.*, 2002; *de Villiers*, 2003] may influence foraminiferal Mg/Ca.

[4] Several efforts have been made to correct the foraminiferal Mg/Ca ratios for the effect of dissolution. For example, *Rosenthal and Lohmann* [2002] established dissolution-corrected Mg/Ca versus temperature calibrations for *Globigerinoides ruber* and *Globigerinoides sacculifer*, based on shell mass loss studies along depth transects, where the preexponential constant is a function of size-normalized shell weight. In an alternative core-top study along depth transects, *Dekens et al.* [2002] introduced water depth-dependent dissolution cor-

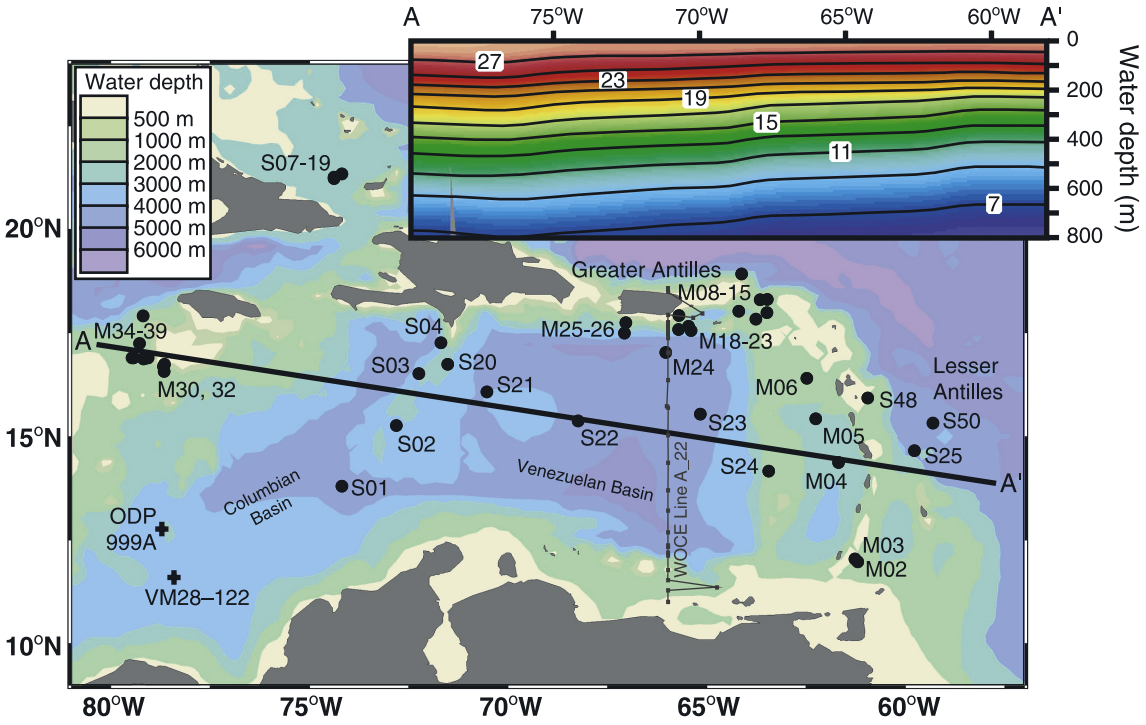

Figure 1. Bathymetric chart of the Caribbean [*Schlitzer*, 2002] showing the locations of the core-top samples from this study (black dots, station labels abbreviate the cruise stations: S: SO164-. . .; M: M35/1, M350. . .) and of two sediment cores (crosses) [*Schmidt et al.*, 2004] discussed here. Inlet presents the annual mean temperature [*NODC*, 2001] versus water depth along the profile AA′. WOCE Line A22 stations are used to compute the carbonate ion concentration considered to be representative for the Caribbean.

rection factors into the exponent of their Mg/Ca versus temperature calibrations for *G. ruber*, *G. sacculifer*, and *Neogloboquadrina dutertrei*, differentiated into Atlantic and Pacific equations. Yet only a few core-top studies covered the upper 2000 m of the water column to a larger extent.

[5] Our study focusses on the impact of water depth-related partial calcite dissolution on the Mg/Ca ratios of seven planktonic foraminiferal species and four of their varieties from water depths of ~900–4700 m. All selected foraminifers were collected from core-top sediments from the Caribbean and the adjacent tropical Atlantic (Figure 1). The thermal structure in the study area minimizes temperature-induced variability in the foraminiferal Mg/Ca, and allows to isolate the impact of calcite dissolution. Our results indicate that Mg/Ca remains stable down to species-specific water depths.

2. Hydrography

[6] Although seasonal variability influences the strength of the trade winds and current patterns in the Caribbean [*Schott et al.*, 1988; *Molinari et al.*, 1990; *Morrison and Smith*, 1990; *Larsen*, 1992; *Johns et al.*, 2002], seasonal temperature changes are relatively small. Within the mixed layer, spatial temperature gradients at similar water depths are in the order of 1°C, increasing to ~4°C within the thermocline [*National Oceanographic and Data Center (NODC)*, 2001] (Figure 1).

[7] The Upper North Atlantic Deep Water (UNADW) with salinity values of 34.7–34.9 [*Wüst*, 1963; *Joyce et al.*, 1999; *Schmuker and Schiebel*, 2002] ventilates the Columbian and Venezuelan Basins via the Greater Antilles Passages [*Stalcup et al.*, 1975; *Morrison and Nowlin*, 1982; *Fratantoni et al.*, 1997]. Above the UNADW, Antarctic Intermediate Water (AAIW) enters the Caribbean between ~550–1000 m [*Wüst*, 1963; *Bulgakov and Lomakin*, 1995; *Schmuker and Schiebel*, 2002]. AAIW mixes with overlying Subtropical Under Water (SUW), forming the permanent thermo- and nutricline in the Caribbean [*Kameo*, 2002]. The SUW with salinity values of >36.8 [*Corredor and Morell*, 2001; *Schmuker and Schiebel*, 2002] and temper-

Table 1. Locations, Depths, and Ages of Core Top Samples of This Study[a]

Station	Longitude, W	Latitude, N	Water Depth *d*, m	Sample, cm	^{14}C Age, years BP	Lab. Number	2 Sigma Age Ranges, years BP	Marine Reservoir Correction (ΔR), years
M35006-6	62°27.2′	16°25.3′	888	0–1				
M35013-3	63°27.0′	18°18.9′	899	0–1				
SO164-04-2	71°39.09′	17°16.38′	1,013	0–1				
M35038-1	79°13.8′	17°15.7′	1,066	0–1				
M35012-6	63°37.6′	18°18.3′	1,121	0–1				
M35039-1	79°08.7′	17°55.6′	1,142	0–1				
M35023-4	65°41.0′	17°36.2′	1,183	0–1				
M35037-1	79°23.3′	16°54.8′	1,190	0–1				
M35023-3	65°40.9′	17°36.2′	1,192	0–1				
M35036-3	79°25.3′	16°55.0′	1,196	0–1				
M35034-3	79°03.5′	16°54.2′	1,212	0–1				
M35015-1	63°27.1′	17°59.6′	1,230	0–1				
M35035-1	79°07.9′	16°53.6′	1,252	0–1				
SO164-48-2	60°55.0′	15°57.02′	1,286	0–1				
M35030-1	78°36.6′	16°45.3′	1,298	0–1				
M35003-6	61°14.7′	12°05.1′	1,299	0–1				
M35032-1	78°36.9′	16°35.3′	1,363	0–1				
M35002-1	61°10.6′	12°01.9′	1,506	0–1				
SO164-24-3	63°25.43′	14°11.89′	1,545	0–1				
M35014-1	63°44.2′	17°50.5′	1,604	0–1				
SO164-18-1	74°21.0′	21°13.61′	1,629	0–1	1,350 ± 25	KIA23386	774–924	37 ± 14
SO164-19-3	74°20.98′	21°14.7′	1,706	0–1	> AD 1954	KIA23383		
M35018-1	65°22.2′	17°34.5′	1,728	0–1				
M35025-1	67°00.5′	17°45.2′	1,778	0–1	699 ± 30	[b]	280–445	−16 ± 23
M35019-1	65°26.1′	17°40.3′	1,815	0–1				
M35020-2	65°40.2′	17°55.8′	2,005	0–1				
M35005-3	62°13.9′	15°27.2′	2,289	0–1				
M35010-2	64°05.4′	18°56.0′	2,696	0–1				
SO164-25-3	59°44.48′	14°41.25′	2,720	0–1	1,915 ± 30	KIA23385	1,287–1,577	33 ± 60
SO164-07-3	74°08.76′	21°19.46′	2,722	0–1	720 ± 35	KIA23384	262–423	37 ± 14
SO164-03-3	72°12.31′	16°32.40′	2,744	0–1				
M35008-1	64°09.8′	18°01.9′	2,820	0–1				
M35004-1	61°39.7′	14°24.6′	2,885	0–1				
SO164-02-3	72°47.06′	15°18.29′	2,977	0–1	2,205 ± 25	KIA23382	1,717–1,914	−16 ± 23
SO164-20-2	71°29.22′	16°45.49′	3,357	0–1				
M35026-2	67°02.6′	17°30.5′	3,815	0–1	1,175 ± 70	[b]	628–900	−16 ± 23
SO164-21-3	70°30.0′	16°06.0′	3,995	0–1				
SO164-50-3	59°16.94′	15°21.25′	4,002	0–1				
SO164-01-3	74°09.028′	13°50.195′	4,026	0–1				
SO164-23-3	65°08.09′	15°34.01′	4,328	0–1				
SO164-22-2	68°12.0′	15°24.0′	4,506	0–1				
M35024-6	66°00.1′	17°02.6′	4,710	0–1	2,510 ± 45	[b]	2,059–2,318	−16 ± 23

[a] The ^{14}C ages are calibrated after *Stuiver et al.* [2005]. Marine reservoir corrections after *Reimer et al.* [2004].
[b] From *Schmuker* [2000].

atures of 18–23°C [*Morrison and Nowlin*, 1982] ranges between ~80–180 m [*Wüst*, 1964] or even down to ~300 m [*Schmuker and Schiebel*, 2002] (Figure 3). It emanates from the North Atlantic subtropical gyre and enters the Caribbean via the Greater Antilles Passages [*Wüst*, 1964; *Johns et al.*, 2002]. The mixed layer is composed of Caribbean Water (CW) in the upper ~80 m of the water column with salinity values of ~35.5 and temperatures of ~28°C [*Wüst*, 1964; *Corredor and Morell*, 2001] (Figure 3).

3. Materials and Methods

3.1. Core-Top Sediments

[8] Mg/Ca analyses were performed on tests of planktonic foraminiferal species or their varieties

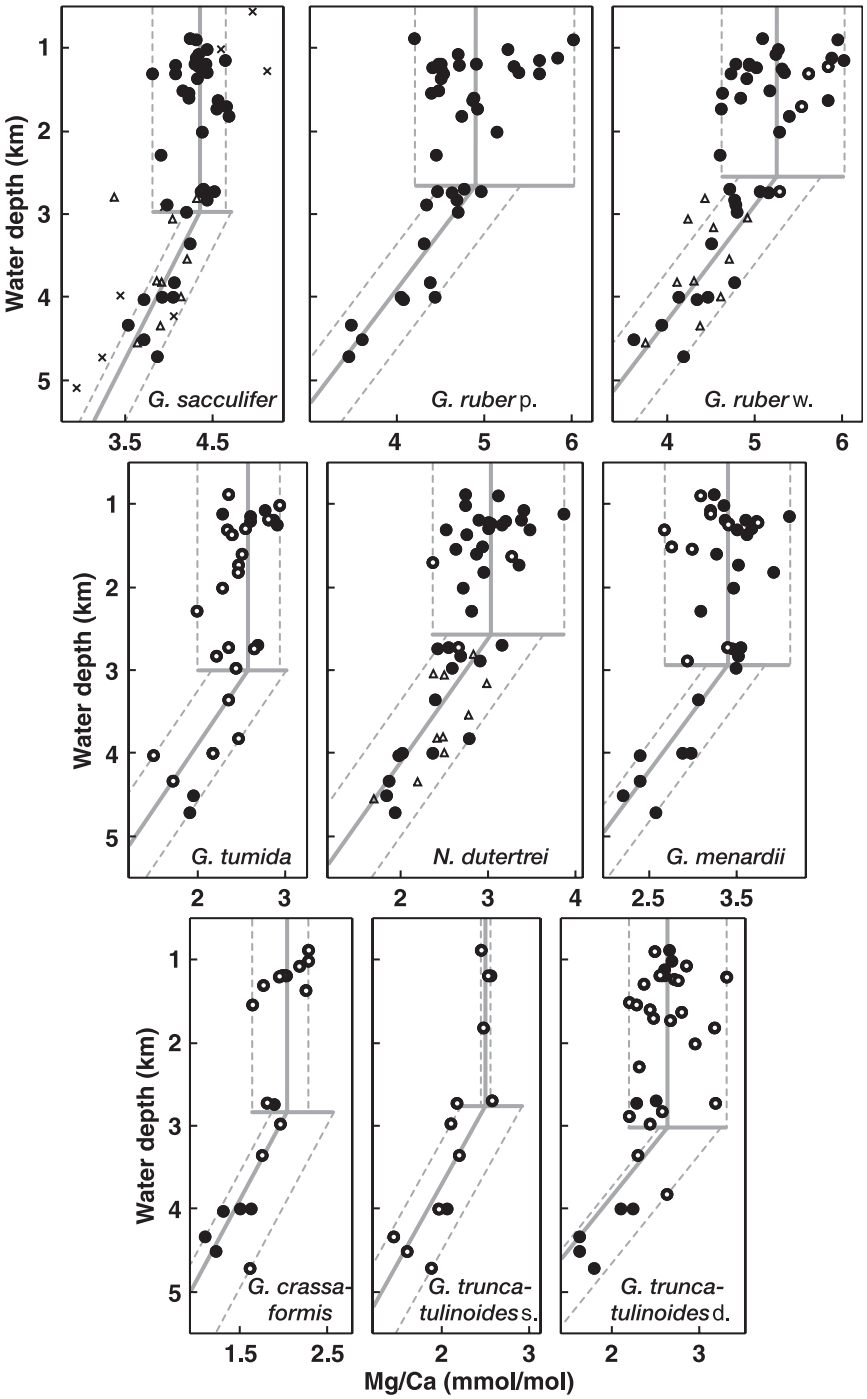

Figure 2. Mg/Ca ratios (black dots from 355–400 μm size fraction; open circles from enlarged size fractions; see Table 2) versus water depth for each planktonic foraminiferal species or variety. The data show significant decreases below species-specific water depth levels ($d_{critical}$ = horizontal line). $d_{critical}$ is defined as the intercept between the vertical (species-specific mean Mg/Ca calculated from samples <2000 m water depth (Table 2)) and diagonal lines (regression lines from Mg/Ca from >3000 m water depth). Below $d_{critical}$, the intraspecific scatter in Mg/Ca is significantly reduced. The dashed lines mark envelopes of measured Mg/Ca. For comparison, Mg/Ca of *Rosenthal et al.* [2000] (crosses) and *Dekens et al.* [2002] (triangles) are included. As the data of *Dekens et al.* [2002] are based on a foraminiferal cleaning protocol involving the reductive hydrazine step, we added 15% to their original Mg/Ca data according to the instructions of *Rosenthal et al.* [2004].

from 42 sediment surface samples (0–1 cm; Figure 1; Table 1), collected during R/V SONNE SO164 [*Nürnberg et al.*, 2003] and R/V METEOR M35/1 cruises [*Zahn et al.*, 1996]. On the basis of 7 AMS^{14}C-dated core tops revealing ages not older than 2–3 kyrs (Table 1), we assume the remaining core-top sediments to be within the same age range.

[9] Twenty to 25 visually (magnification up to 40×) uncontaminated tests of the foraminiferal species or their varieties were selected from the narrow 355–400 μm size fraction (~550–800 μg) for Mg/Ca analyses to minimize size-related intraspecific elemental variations [*Elderfield et al.*, 2002]. In case of insufficient material, we subsequently extended the selection of tests to a larger size range (maximum 250–500 μm; Figure 2; Table 2).

3.2. Foraminiferal Species Selection

[10] Seven tropical to subtropical planktonic foraminiferal species and four of their varieties were selected for Mg/Ca analyses. Generic assignments of selected specimens in this study follow *Kennett and Srinivasan* [1983] and *Hemleben et al.* [1989]. The specific adaptations to and demands of light, chlorophyll concentrations, salinity, temperature, and food availability [e.g., *Fairbanks et al.*, 1980, 1982; *Fairbanks and Wiebe*, 1980; *Curry et al.*, 1983; *Deuser*, 1987; *Deuser and Ross*, 1989; *Sautter and Thunell*, 1991a; *Ortiz et al.*, 1995, 1996, 1997; *Watkins and Mix*, 1998] determine the vertical distribution patterns and abundances of planktonic foraminiferal species in the water column. Their different preferred depth habitats thus allow the reconstruction of the upper ocean structure in detail, presupposing that the various foraminiferal habitats remain fixed through time and environmental change.

[11] *G. ruber* and *G. sacculifer* are spinose and symbiont-bearing species. They commonly reach highest abundances in the upper 50 m of the mixed layer [*Bé*, 1977; *Fairbanks et al.*, 1982; *Deuser*, 1987; *Bijma et al.*, 1994; *Kroon and Darling*, 1995; *Kemle-von Mücke and Oberhänsli*, 1999; *Schmuker and Schiebel*, 2002]. An almost uniform occurrence throughout the year makes *G. ruber* suitable to reflect annual hydrographic conditions [*Hemleben et al.*, 1989; *Lin et al.*, 1997; *Tedesco and Thunell*, 2003]. *Savin and Douglas* [1973] showed that *G. ruber* calcifies at shallower water depths than *G. sacculifer*.

[12] *Globorotalia menardii* and *N. dutertrei* live within the tropical to subtropical thermocline [*Ravelo and Fairbanks*, 1992; *Chaisson and Ravelo*, 1997]. *N. dutertrei* is known to occur in a well-stratified photic zone near the deep chlorophyll maximum [*Fairbanks et al.*, 1980, 1982; *Fairbanks and Wiebe*, 1980], often associated with the lower thermocline [*Sautter and Thunell*, 1991a; *Ravelo and Fairbanks*, 1992].

[13] *Globorotalia tumida* calcifies near the bottom of the photic zone [*Ravelo and Fairbanks*, 1992; *Chaisson and Ravelo*, 1997]. It shows distinct preferences for low water densities during summer [*Hilbrecht*, 1996]. *Globorotalia truncatulinoides* and *Globorotalia crassaformis* are deep-dwelling species that reach maximum abundances below the photic zone [*Ganssen and Kroon*, 2000]. According to *Mulitza et al.* [1997], *G. truncatulinoides* reflects mean ocean conditions at about 200 m, while *McKenna and Prell* [2004] assign the habitat to the permanent thermocline. In the Caribbean, *G. truncatulinoides* is linked to the SUW [*Schmuker*, 2000]. Changing coiling directions do not indicate substantially different physical preferences [*Hilbrecht*, 1996]. *G. crassaformis* calcifies below the photic zone and thermocline [*Ravelo and Fairbanks*, 1992]. In general, *G. crassaformis* is supposed to behave like *G. truncatulinoides* [*Hemleben et al.*, 1989].

[14] Impending gametogenesis is morphologically signaled by additional calcification of a diminutive final chamber for *G. ruber* [*Bijma et al.*, 1990], a sac-like final chamber for *G. sacculifer* [*Bé et al.*, 1983; *Hemleben et al.*, 1989], and by discarding of spines [*Bé*, 1980; *Duplessy et al.*, 1981]. Secondary calcite crust formation, associated with reproduction, mainly occurs at greater depths [*Hemleben et al.*, 1989; *Lohmann*, 1995], and hence may affect the geochemical signature of the foraminiferal tests [e.g., *Curry and Crowley*, 1987; *Spero and Williams*, 1989; *Lohmann*, 1995; *Nürnberg et al.*, 1996a; *Rosenthal et al.*, 2000; *Eggins et al.*, 2003; *Mulitza et al.*, 2003; *McKenna and Prell*, 2004]. Addition of secondary calcite accounts for about one third of the test's mass of *G. sacculifer* [*Bé*, 1980; *Erez and Honjo*, 1981; *Hemleben et al.*, 1989; *Schweitzer and Lohmann*, 1991; *Bijma et al.*, 1994], and doubles the test's mass of *G. truncatulinoides* [*Bé and Lott*, 1964]. Large vertical migrations during their ontogenetic cycles were described for *G. menardii*, *G. tumida*, and *G. truncatulinoides* [*Bé and Ericson*, 1963; *Bé*,

Table 2. Measured Mg/Ca Ratios and Size Fractions of Selected Specimens[a]

Station	*d*, m	*G. ruber* p.	*G. ruber* w.	*G. sacculifer*	*N. dutertrei*	*G. menardii*	*G. tumida*	*G. truncatulinoides* d.	*G. truncatulinoides* s.	*G. crassaformis*
M35006-6	888	a 4.20	a 5.09	a 4.23	a 2.73	a 3.24	d 2.35	a 2.65	d 2.45	b 2.28
M35013-3	899	a 6.02	a 5.95	a 4.31	a 3.11	d 3.09		d 2.48		
SO164-04-2	1,013	a 5.26	a 5.27	a 4.43	a 2.74	a 3.35	i 2.93	c 2.68		b 2.28
M35038-1	1,066	a 4.70	a 5.23	a 4.34	a 3.41	a 3.20	a 2.76	g 2.85		g 2.18
M35012-6	1,121	a 5.84	a 5.87	a 4.31	a 3.87	i 3.20	a 2.27	a 2.59		
M35039-1	1,142	a 5.62	a 6.02	a 4.64	a 5.59[b]	a 4.10[c]	a 2.59	a 5.80[b]		
M35023-4	1,183	a 4.50						a 2.58	d 2.53	f 2.04
M35037-1	1,190	a 4.91	a 4.94	a 4.41	a 2.89	a 3.36	e 2.80	g 2.55		e 2.01
M35023-3	1,192	a 4.48	a 4.77	a 4.29	a 3.37	a 3.60	a 2.87	a 2.60	e 2.55	a 1.97
M35036-3	1,196	a 4.714	a 4.929	a 4.066	a 3.192	a 3.728	a 2.594	g 3.304		e 1.94
M35034-3	1,212	a 5.34	b 5.84	a 4.34	a 3.00	b 3.74				
M35015-1	1,230	a 4.41	a 5.01	a 4.39	a 3.03	c 3.41		c 2.71		
M35035-1	1,252	a 4.50	a 5.30	a 4.41	a 3.16	a 3.40	a 2.90	h 2.75		
SO164-48-2	1,286	a 5.39	a 5.33	a 4.43	a 3.00	a 3.66	c 2.55	c 2.36		
M35030-1	1,298	a 5.62	b 5.61	a 4.07	a 3.47	a 3.51	d 2.33			
M35003-6	1,299	a 4.53	a 4.72	a 3.80	a 2.51	e 2.67				e 1.77
M35032-1	1,363	a 4.51	a 4.91	a 4.33	a 2.75	a 3.61	c 2.40			d 2.26
M35002-1	1,506	a 4.47	a 5.17	a 4.15	a 2.93	c 2.75		d 2.20		
SO164-24-3	1,545	a 4.39	a 4.63	a 4.23	a 2.63	j 2.98		c 2.28		c 1.64
M35014-1	1,604	a 4.88	a 4.83	a 4.23	a 2.86	a 3.26	d 2.50	d 2.44		
SO164-18-1	1,629	a 4.86	a 5.83	a 4.55	b 3.27			b 2.79		
SO164-19-3	1,706		e 5.53	a 4.65	e 2.36			c 2.48		
M35018-1	1,728	a 4.91	a 4.62	a 4.54	a 3.35	a 3.51	c 2.46	c 2.67		
M35019-1	1,815	a 4.73	a 5.39	a 4.68	a 2.95	a 3.92	b 2.46	b 3.17	d 2.47	
M35020-2	2,005	a 5.14	a 5.28	a 4.38	a 2.71	a 3.45	c 2.28	b 2.95		
M35005-3	2,289	a 4.45	a 4.59	a 3.90	a 2.81	a 3.08	d 1.99	d 2.30		
M35010-2	2,696	a 4.77	a 4.70	a 4.38	a 3.15	a 4.66[c]	a 2.69	a 2.50	b 2.57	
SO164-25-3	2,720	a 4.46	a 5.05	a 4.36	a 2.55	a 3.54	b 2.35	a 2.28	c 2.17	c 1.81
SO164-07-3	2,722	a 4.96	b 5.28	a 4.51	b 2.66	c 3.39		c 3.19		
SO164-03-3	2,744	a 4.62	a 5.15	a 4.44	a 2.42	a 3.44	c 2.64			a 1.89
M35008-1	2,820	a 4.68	a 4.77	a 4.43	a 2.68	a 3.51	d 2.20	b 2.57		
M35004-1	2,885	a 4.34	a 4.78	a 3.98	a 2.91	c 2.94		b 2.20		
SO164-02-3	2,977	a 4.70	a 4.79	a 4.20	a 2.58	a 3.49	c 2.43	c 2.43	c 2.10	b 1.96
SO164-20-2	3,357	a 4.30	a 4.51	a 4.23	a 2.39	a 3.05	b 2.35	b 2.30	c 2.20	b 1.76
M35026-2	3,815	a 4.37	a 4.76	a 4.06	a 2.78	a 3.99[c]	d 2.46	g 2.62		
SO164-21-3	3,995	a 4.44	a 4.45	a 4.04	a 2.36	a 2.88	b 2.17	a 2.24	b 1.96	a 1.63
SO164-50-3	4,002	a 4.04	a 4.13	a 3.92	a 2.02	a 2.98	i 2.17	a 2.10	a 2.05	a 1.50
SO164-01-3	4,026	a 4.07	a 4.34	a 3.71	a 1.98	a 2.40	h 1.48			a 1.31
SO164-23-3	4,328	a 3.47	a 3.93	a 3.53	a 1.87	a 2.38	i 1.72	a 1.63	c 1.45	a 1.09
SO164-22-2	4,506	a 3.60	a 3.62	a 3.71	a 1.84	a 2.20	a 1.95	a 1.62	c 1.60	a 1.23
M35024-6	4,710	a 3.44	a 4.19	a 3.86	a 1.93	a 2.56	a 1.91	a 1.79	e 1.88	e 1.61
Mg/Ca_{mean}		4.9	5.25	4.34	3.03	3.36	2.58	2.64	2.5	2.04

Table 2. (continued)

Station	*d*, m	*G. ruber* p.	*G. ruber* w.	*G. sacculifer*	*N. dutertrei*	*G. menardii*	*G. tumida*	*G. truncatulinoides* d.	*G. truncatulinoides* s.	*G. crassaformis*
sd		0.51	0.44	0.2	0.35	0.32	0.22	0.27	0.05	0.22
Temperature		28.41	29.18	27.06	23.07	24.22	21.28	21.54	20.93	18.67

[a] Each single ratio is the average of three measurements, except the samples listed in Table 3. Mean Mg/Ca (Mg/Ca_{mean}) ± standard deviations (sd) from 2000 m are converted into temperatures after *Anand et al.* [2003] ($Mg/Ca = 0.38 \cdot \exp(0.09T)$). Specimens size fractions: a, 355-400 μm; b, 315-400 μm; c, 315-450 μm; d, 315-500 μm; e, 250-400 μm; f, 250-450 μm, g: 250-500 μm, h: 355-500 μm; i, 355-450 μm; j, 400-500 μm.
[b] Not used for calculation of the mean <2,000 m.
[c] Not considered for the calculation of the linear regression.

1977; *Fairbanks et al.*, 1980, 1982; *Fairbanks and Wiebe*, 1980; *Erez and Honjo*, 1981; *Hemleben et al.*, 1989; *Schweitzer and Lohmann*, 1991; *Brown and Azmy*, 2005].

[15] To prevent our analyses from biases due to different amounts of secondary calcite, we took care upon specimen selection. For *G. ruber* (pink and white varieties) and *G. sacculifer*, tests with spines were preferentially selected. For the latter, specimens showing a sac-like final chamber were excluded. For *G. menardii* and for *G. tumida*, we chose thin-walled and thick-encrusted specimens, respectively. Due to the low numbers of tests of *G. truncatulinoides* (dextral and sinistral varieties) and *G. crassaformis*, we did not differentiate between encrusted and nonencrusted specimens, and different morphotypes. In general, specimens with kummerform chambers were rejected.

3.3. Mg/Ca Analyses

[16] The foraminiferal samples were cleaned according to the cleaning protocol of *Barker et al.* [2003]. Prior to cleaning, the tests were gently crushed between two glass plates in order to open all chambers. The foraminiferal fragments were rinsed 5 times with ultrapure water and twice with methanol (suprapure), including ultrasonic treatment after each rinse. Subsequently, samples were treated twice with 250 μL of a hot (97°C) oxidizing 1% $NaOH/H_2O_2$ reagent (10 mL 0.1 N NaOH (analytical grade); 100 μL 30% H_2O_2 (suprapure)) for 10 minutes. Every 2.5 minutes, the solution was cautiously agitated in order to release any gaseous build-up. After 5 minutes, the samples were placed in an ultrasonic bath for a few seconds in order to maintain the chemical reaction. Remaining oxidizing solution was removed by three rinsing steps with ultrapure water. After transferring the samples into clean vials, a weak acid leach with 250 μL 0.001 M nitric acid (HNO_3, subboiled distilled) was applied with 30 seconds ultrasonic treatment, followed by two rinses with ultrapure water. After removal of any remaining solution, the samples were dissolved in 500 μL 0.075 M HNO_3 (subboiling distilled), and diluted with ultrapure water to achieve Ca concentrations of 30–70 ppm.

[17] Analyses were performed on two ICP OES devices showing no significant offset as revealed by replicate measurements of 21 samples (Table 3). Each single Mg/Ca ratio (Tables 2 and 3) is the average of three measurements, from which the analytical errors are deduced. One set of samples was measured on an ICP OES (ISA Jobin Yvon,

Table 3. Replicate Mg/Ca Measurements on Two ICP OES Devices[a]

Station	Species	Mg/Ca, mmol/mol ISA Jobin Yvon		Mg/Ca, mmol/mol Spectro Ciros			Mg/Ca, mmol/mol	
		1	2	1	2	3	Mean	sd
SO164-22-2	*G. crassaformis*			* 1.22	* 1.23		1.23	0.00
SO164-04-2	*G. crassaformis*			* 2.29	* 2.28		2.28	0.00
SO164-02-3	*G. crassaformis*			* 2.07	** 1.85		1.96	0.08
SO164-01-3	*G. crassaformis*			* 1.32	** 1.30		1.31	0.01
M35018-1	*G. menardii*			* 3.31	** 3.72		3.51	0.29
M35037-1	*G. menardii*			* 3.53	** 3.20		3.36	0.23
M35036-3	*G. menardii*			* 3.81	** 3.28	*** 4.09	3.73	0.41
SO164-20-2	*G. ruber* p.			* 4.30	* 4.30		4.30	0.00
SO164-02-3	*G. ruber* p.			* 4.81	** 4.59		4.70	0.08
SO164-18-1	*G. ruber* p.			* 4.87	* 4.85		4.86	0.00
SO164-25-3	*G. ruber* w.	* 4.75		* 5.35			5.05	0.21
SO164-23-3	*G. ruber* w.	* 3.58		** 4.33	*** 3.87		3.93	0.25
SO164-04-2	*G. ruber* w.	* 5.34		** 5.20			5.27	0.05
SO164-01-3	*G. ruber* w.	* 4.38		* 4.41	** 4.22		4.34	0.10
SO164-19-3	*G. ruber* w.	* 5.75		* 5.32			5.53	0.15
SO164-48-2	*G. sacculifer*			* 4.48	* 4.38		4.43	0.03
SO164-24-3	*G. sacculifer*	* 4.10		** 4.36			4.23	0.09
M35014-1	*G. sacculifer*			* 4.36	** 4.09		4.23	0.19
SO164-23-3	*G. sacculifer*	* 3.41		** 3.66	*** 3.52		3.53	0.08
SO164-22-2	*G. sacculifer*	* 3.90		** 3.53			3.71	0.13
M35037-1	*G. sacculifer*			* 4.39	** 4.44		4.41	0.04
SO164-50-3	*G. truncatulinoides* d.			* 2.14	** 2.07		2.10	0.02
SO164-48-2	*G. truncatulinoides* d.			* 2.35	** 2.27		2.31	0.03
M35023-4	*G. truncatulinoides* d.			* 2.59	** 2.56		2.58	0.02
M35023-4	*G. truncatulinoides* s.			* 2.41	** 2.65		2.53	0.17
SO164-50-3	*G. tumida*			* 2.17	* 2.16		2.17	0.01
SO164-25-3	*G. tumida*			* 2.36	* 2.35		2.35	0.00
SO164-48-2	*G. tumida*			* 2.55	* 2.54		2.55	0.00
SO164-23-3	*G. tumida*			* 1.64	* 1.64	** 1.87	1.72	0.12
SO164-22-2	*G. tumida*			* 1.96	* 1.94		1.95	0.01
SO164-20-2	*G. tumida*			* 2.35	* 2.35		2.35	0.00
SO164-03-3	*G. tumida*			* 2.66	* 2.63		2.64	0.01
SO164-02-3	*G. tumida*			* 2.44	* 2.43		2.43	0.00
SO164-01-3	*G. tumida*			* 1.49	* 1.48		1.48	0.00
SO164-50-3	*N. dutertrei*	* 1.99		* 2.05			2.02	0.02
SO164-25-3	*N. dutertrei*	* 2.49		* 2.60			2.55	0.04
SO164-48-2	*N. dutertrei*	* 3.30	** 2.85	* 3.17	** 2.84	** 2.87	3.00	0.19
SO164-23-3	*N. dutertrei*	* 1.84		* 1.89			1.87	0.02
SO164-22-2	*N. dutertrei*	* 1.82	** 1.87	* 1.82	** 1.85		1.84	0.02
SO164-21-3	*N. dutertrei*	* 2.38	* 2.33				2.36	0.02
SO164-20-2	*N. dutertrei*	* 2.55		* 2.35	* 2.36		2.42	0.04
SO164-04-2	*N. dutertrei*	* 2.74		* 2.73			2.74	0.00
SO164-03-3	*N. dutertrei*	* 2.38		* 2.47			2.42	0.03
SO164-02-3	*N. dutertrei*	* 2.57		* 2.59			2.58	0.01
SO164-01-3	*N. dutertrei*	* 1.91	** 1.99	* 1.95	** 2.07		1.98	0.05
SO164-07-3	*N. dutertrei*	* 2.62		* 2.69			2.66	0.02
SO164-19-3	*N. dutertrei*	* 2.32		* 2.40			2.36	0.03
SO164-18-1	*N. dutertrei*	* 3.28		* 3.26			3.27	0.01

[a] The use of same sample solutions is indicated by asterisks.

Spex Instruments S.A. GmbH) with polychromator applying yttrium as an internal standard. Selected element lines for analyses (Ca: 317.93 nm; Mg: 279.55 nm; Y: 371.03 nm) were most intensive and undisturbed. Element detection was performed with photomultipliers, the high-tension of which was adapted to each element concentration range. The analytical error for Mg is ~0.45% and for Ca ~0.15%. Replicate samples showed an average standard deviation of ~0.1 mmol/mol (Table 3). A second set of samples was measured on a simultaneous, radially viewing ICP OES (Spectro

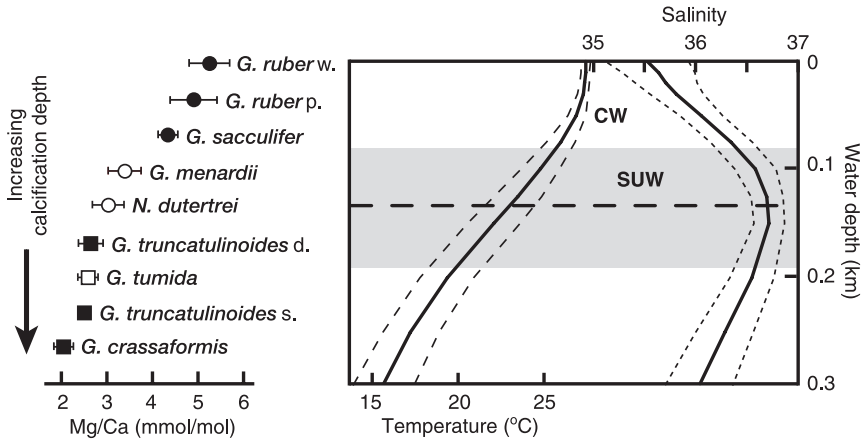

Figure 3. Species-specific mean Mg/Ca ratios from <2000 m water depth (error bars indicate standard deviations) ranked from highest to lowest Mg/Ca versus relative calcification depth. Black dots: shallow-dwelling species; circles: thermocline-dwelling species; open square: bottom-of-photic-zone-dwelling species; black squares: deep-dwelling species. For comparison, eastern Caribbean annual mean temperatures and salinities (±standard deviations) [*NODC*, 2001] versus water depth are shown. Shaded area indicates the thermocline. Horizontal dashed line marks the base of the photic zone (inferred from the irradiance value of 0.1%). CW, Caribbean Water; SUW, Subtropical Underwater.

CirosCCD SOP). A cooled cyclonic spraychamber in combination with a microconcentric nebulizer (200 μL/min sample uptake) was optimized for best precision of analytical results and minimized uptake of sample solution. Sample introduction took place via autosampler (Spectro A.I.). For Ca, we used the spectral line with the highest stability (183.801 nm). For Mg, we used the most sensitive line (279.553 nm). Matrix effects caused by varying concentrations of Ca were cautiously checked and found to be insignificant. Drift of the machine during analytical sessions was negligible (<0.5%, as determined by analysis of an internal consistency standard after every 5 samples). The analytical error for the Mg/Ca analyses was ~0.1%. Replicate samples showed an average standard deviation of ~0.08 mmol/mol (Table 3).

4. Results and Discussion

4.1. Bathymetric Change in Mg/Ca Ratios

[18] For all foraminiferal species and varieties studied, we observe a considerable decrease in Mg/Ca ratios with increasing water depth below certain depth levels. Depending on the species or variety, the change from stable to continuously decreasing Mg/Ca happens in the depth range between ~2000 m and ~3000 m. Statistical analyses of the intraspecific Mg/Ca reveal that means of samples from <2000 m water depth differ significantly from those from >2000 m. Related low probability values ($p < 0.015$) of these Mg/Ca means indicate that both data sets behave significantly different and that environmental factors other than temperature bias Mg/Ca at deeper sites. According to the bathymetric distribution of the core-top samples in combination with the pattern of the Mg/Ca data (Figure 2), we assign decreasing Mg/Ca to dissolution and differentiate between three water depth intervals: (1) samples <2000 m with no signs of preferential removal of Mg^{2+} (number of core-top samples n = 23; Table 3), (2) samples >3000 m with distinctively decreasing Mg/Ca (n = 8; Table 3), and (3) samples between 2000–3000 m (n = 9; Table 3). The incomplete distribution pattern of the latter sample set prevents to directly infer the transition depth separating Mg/Ca unaffected and affected by dissolution, respectively.

4.2. Dissolution Unaffected Mg/Ca Ratios From Shallow Water Depths

[19] Evidence for excellent carbonate preservation at shallow water depths is provided by the presence of aragonitic pteropod shells in our Caribbean core-top sediments down to ~2700 m. Likewise, species-specific Mg/Ca ratios do not systematically decrease with increasing water depth in the depth interval <2000 m (correlation coefficients r^2 = <0.1). We assume these shallow Mg/Ca to be unaffected by dissolution.

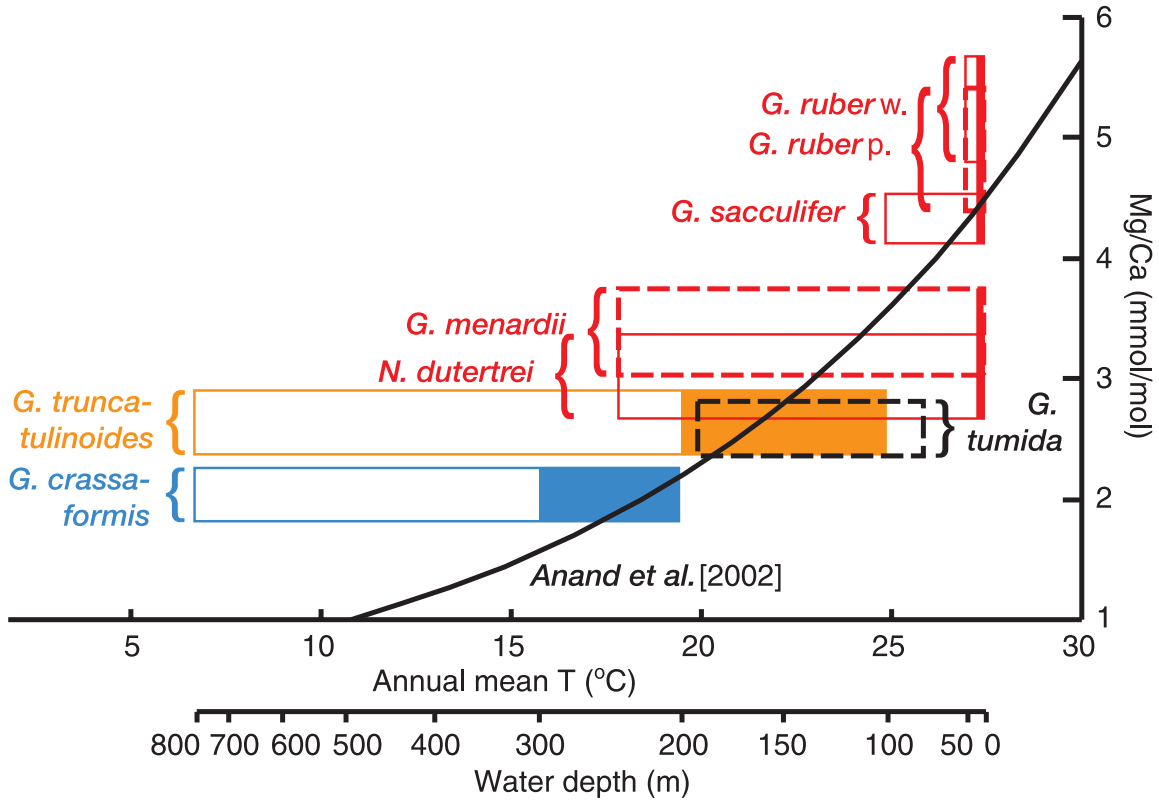

Figure 4. Species-specific mean Mg/Ca ratios from <2000 m water depth (box heights indicate Mg/Camean ± standard deviations) versus eastern Caribbean annual temperatures [*NODC*, 2001]. The eastern Caribbean annual temperatures were converted from the according habitat depths compiled for the different species and their varieties (widths of open and filled boxes; see section 4.3). Considering only those habitat specifications (filled boxes) derived from eastern Caribbean plankton tows [*Schmuker and Schiebel*, 2002] (0–20 m (red bars); 100–200 m (orange bar); 200–300 m (blue bar)), the Mg/Ca versus temperature relationship comes close to the multispecies calibration curve of *Anand et al.* [2003] (black curve).

[20] There are significant differences in Mg/Ca ratios between the species and varieties from <2000 m (Figure 2; Table 2). Mixed layer-dwelling *G. ruber* exhibits highest Mg/Ca of 4.20–6.02 mmol/mol. In accordance with increasing calcification depth and decreasing ambient seawater temperature, Mg/Ca successively decrease to 1.64–2.28 mmol/mol for the deepest-living species *G. crassaformis* (Figure 2). With respect to *G. ruber*, the other species show lower mean Mg/Ca in samples <2000 m water depth (Figure 3): *G. sacculifer* is lower in Mg/Ca by ~15%, *G. menardii* by ~34%, *N. dutertrei* by ~40%, *G. tumida* by ~49%, *G. truncatulinoides* by ~49%, and *G. crassaformis* by ~60%. *G. ruber* pink shows consistently lower mean Mg/Ca from <2000 m by ~7% with respect to the white variety. The left-coiling variety of *G. truncatulinoides* (sinistral) is lower by ~5% with respect to the right-coiling (dextral) variety (Figures 2 and 3). These differences between species are in general agreement to previous multispecies core-top studies of *Hecht et al.* [1975], *Lorens et al.* [1977], *Rosenthal and Boyle* [1993], *Russell et al.* [1994], *Brown and Elderfield* [1996], *Hastings et al.* [1996], *Dekens et al.* [2002], and *Anand et al.* [2003] (Figure 2).

4.3. Temperature Versus Mg/Ca Ratios Unaffected by Dissolution

[21] The accuracy of Mg/Ca versus temperature calibration curves depends on both the accuracy of Mg/Ca analyses and, more importantly, on the accuracy of the temperature assignment. The temperature assignment, however, is dependent on the foraminiferal habitat (e.g., water depth, season, life cycle, nutrient supply), which often comprises a broad range of water depths wherein calcification takes place. In Figure 4, we plotted the foraminiferal Mg/Ca ratios from <2000 m versus Caribbean annual mean temperatures [*NODC*, 2001]. These temperatures were converted from the specific

foraminiferal habitat assignments found in the literature [*Fairbanks et al.*, 1980, 1982; *Fairbanks and Wiebe*, 1980; *Erez and Honjo*, 1981; *Hemleben et al.*, 1989; *Sautter and Thunell*, 1991a; *Schweitzer and Lohmann*, 1991; *Ravelo and Fairbanks*, 1992; *Mulitza et al.*, 1997; *Kemle-von Mücke and Oberhänsli*, 1999; *Schmuker and Schiebel*, 2002; *Anand et al.*, 2003; *McKenna and Prell*, 2004]. Considering only the habitat specifications of *Schmuker and Schiebel* [2002] inferred from abundance maxima of eastern Caribbean plankton tows (April–May 1996), an exponential multispecies Mg/Ca versus temperature relationship suggests itself, which approaches the multispecies calibration curve of *Anand et al.* [2003] established for the Sargasso Sea (Figure 4). The slope of such a calibration curve, however, is highly dependent on the determination of the foraminiferal habitat depths. In fact, while estimates on where foraminifers live and where calcification occurs are manifold or speculative, $\delta^{18}O$ data of primarily shallow-dwelling species indicate that planktonic foraminifera calcify in depth zones that are significantly narrower than the overall vertical distribution of these species implies [*Fairbanks et al.*, 1980]. From Mg/Ca of the thermocline-dwelling species *G. menardii* and *N. dutertrei*, which are lower than those of the shallow-dwelling species *G. ruber* and *G. sacculifer* (Figures 3 and 4), we hypothesize that the potential calcification depths of these species, where the Mg/Ca signal is generated, are clearly deeper than the shallow abundance maxima given by *Schmuker and Schiebel* [2002].

[22] Despite the overall correspondence between foraminiferal Mg/Ca ratios and temperature shown in Figure 4, which heavily relies on assumptions concerning the foraminiferal habitats, we note a broad intraspecific range of Mg/Ca in core-top samples from <2000 m water depth, in accordance to early observations of *Nürnberg* [1995] on the high variability of Mg/Ca in foraminiferal tests. The scatter appears to be largest in shallow- and thermocline-dwelling species with a range of ~1.4 mmol/mol in *G. ruber* white, ~1.8 mmol/mol in *G. ruber* pink, ~0.9 mmol/mol in *G. sacculifer*, ~1.3 mmol/mol in *G. menardii*, and ~1.5 mmol/mol in *N. dutertrei*, and a commonly smaller range in deep-dwelling species of ~0.7 mmol/mol in *G. tumida*, ~1.1 mmol/mol in *G. truncatulinoides* dextral, ~0.1 mmol/mol in *G. truncatulinoides* sinistral, and ~0.7 mmol/mol in *G. crassaformis* (Figure 2). The observed range of core-top Mg/Ca appears high, but is close to other shallow core-top and sediment-trap data from other ocean areas at similar temperatures showing a wide range of Mg/Ca of ~1 mmol/mol [e.g., *Elderfield and Ganssen*, 2000; *Whitko et al.*, 2002; *Anand et al.*, 2003] (Figure 5).

[23] The observed scatter in the core-top Mg/Ca ratios may be due to several reasons: (1) An annual mixed layer temperature range of ~2–3°C at the respective core sites within the mixed layer (i.e., ~30–50 m water depth, assumed habitat of shallow-dwelling species [*Schmuker and Schiebel*, 2002]) and a smaller annual temperature range of only ~1–2°C at intermediate water depths (down to ~230 m water depth, assumed habitat of *G. crassaformis* [*Schmuker and Schiebel*, 2002]) (Figure 5) introduces a potential variability in Mg/Ca of ~0.1–0.4 mmol/mol when applying the Mg/Ca versus temperature equation of *Anand et al.* [2003]. (2) The assumed age range of ~2–3 kyrs for the core-top sediments (see section 3.1) might have introduced a certain variance in Mg/Ca due to short-term climate variations. Indeed, a cooling of Caribbean surface water temperatures of about 2°C during the Little Ice Age [*Watanabe et al.*, 2001] could account for a change in Mg/Ca of ~0.7 mmol/mol. (3) A species-specific size-effect on Mg/Ca generally was avoided by selecting foraminiferal tests from narrow size ranges (see section 3.1; Table 2). Especially for the deep-dwelling species, however, we were forced to widen the size range due to insufficient numbers of specimens for analysis (Table 2). Taking the published deviations from mean Mg/Ca of 12–36% by enlargement of the foraminiferal test sizes [*Elderfield et al.*, 2002; *Anand and Elderfield*, 2005], we estimate the size effect on our Mg/Ca to a maximum of ~0.2–0.7 mmol/mol. (4) The presence of varying amounts of secondary, gametogenic calcite (see section 3.2), which is added to the foraminiferal tests at greater water depths and hence records lower temperatures, biases Mg/Ca toward lower ratios. The quantitative effect on Mg/Ca, however, remains uncertain as we have no control on the amounts of gametogenic calcite. (5) Unintended mixing of morphotypes may have led to a widened scatter in Mg/Ca. Foraminiferal species are known to form different morphotypes showing different geochemical signatures [e.g., *Williams et al.*, 1981; *Deuser and Ross*, 1989]. *Steinke et al.* [2005] presented a statistically significant difference in Mg/Ca for two morphotypes of *G. ruber* white of 0.38 ± 0.30 mmol/mol. In spite of all these factors potentially affecting Mg/Ca, the succession of foraminiferal species and varieties

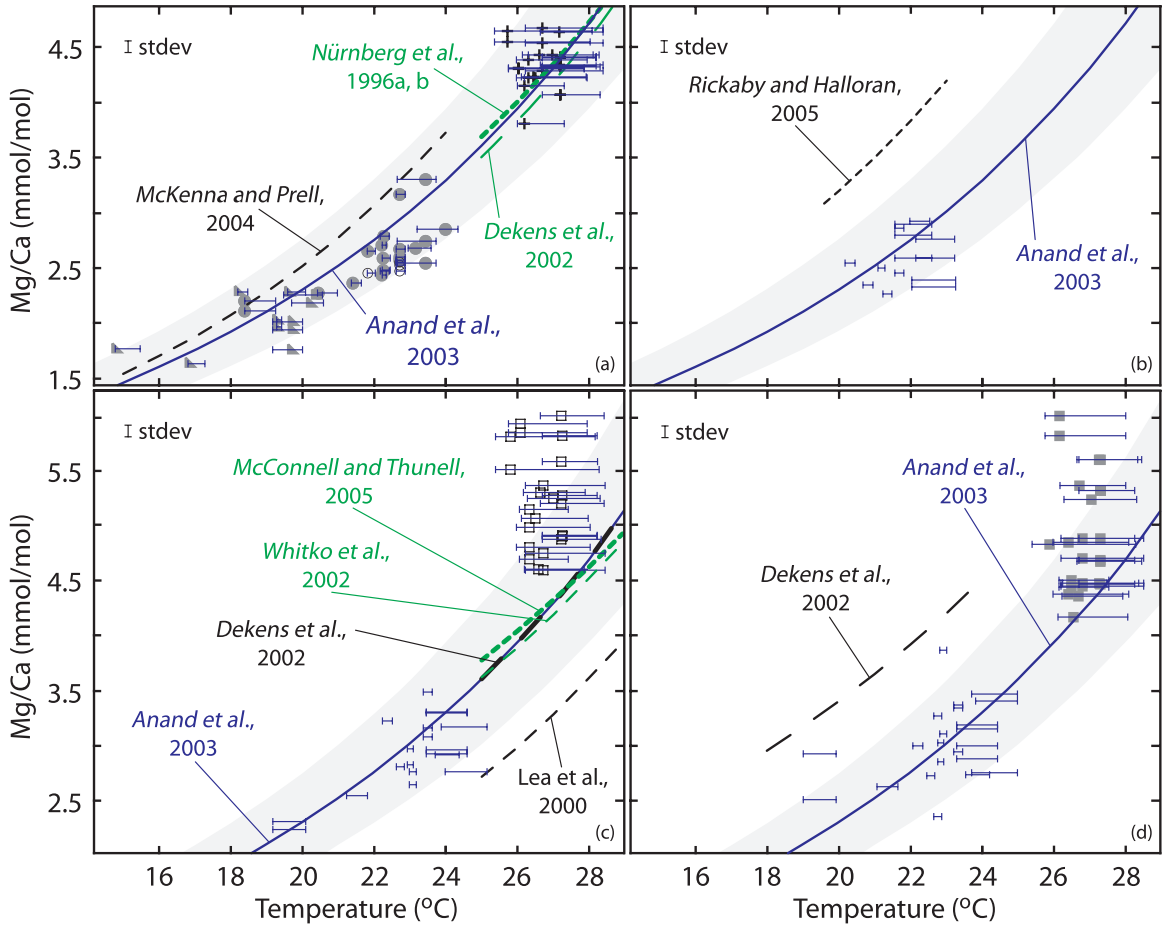

Figure 5. Caribbean core-top Mg/Ca ratios versus temperature data of 9 planktonic foraminiferal species and varieties in comparison with published Mg/Ca-paleotemperature equations. Horizontal bars indicate entire annual temperature ranges [*NODC*, 2001] at the respective core locations from preferred living depths of the foraminiferal species and varieties. Symbols are placed at April-May temperatures when foraminiferal abundance maxima were observed [*Schmuker and Schiebel*, 2002]. Shaded areas indicate the Mg/Ca data variability around the *Anand et al.* [2003] multispecies calibration curve (solid lines: Mg/Ca = 0.38 · exp(0.09T)). Average standard deviations of replicate Mg/Ca analyses (stdev) is indicated by vertical bars. (a) Deep-dwelling *G. crassaformis* (triangles), *G. truncatulinoides* dextral (dots) and sinistral (open circles), and shallow-dwelling *G. sacculifer* (crosses): Habitat depths of ~230 m, ~160 m, and ~40 m, respectively (see section 4.3); species-specific paleotemperature calibration curves for *G. truncatulinoides* dextral from *McKenna and Prell* [2004] (Mg/Ca = 0.355 · exp(0.098T)), and for *G. sacculifer* from *Dekens et al.* [2002] (Mg/Ca = 0.37 · exp(0.09T)) and *Nürnberg et al.* [1996a, 1996b] (Mg/Ca = 0.472 · 10^(0.036T)). (b) Deep-dwelling *G. tumida*: Habitat depth defined to ~180 m; species-specific paleotemperature equation for *G. tumida* from *Rickaby and Halloran* [2005] (Mg/Ca = 0.53 · exp(0.09T)). (c) Thermocline-dwelling *G. menardii* and shallow-dwelling *G. ruber* white (open squares): Habitat depths defined to ~150 m and ~34 m, respectively; species-specific paleotemperature equations for *G. ruber* white from *Lea et al.* [2000] (Mg/Ca = 0.3 · exp(0.09T)), *Dekens et al.* [2002] (Mg/Ca = 0.38 · exp(0.09T)), *Whitko et al.* [2002] (Mg/Ca = 0.57 · exp(0.074T)), and *McConnell and Thunell* [2005] (Mg/Ca = 0.69 · exp(0.068T)). (d) Thermocline-dwelling *N. dutertrei* and shallow-dwelling *G. ruber* pink (squares): Habitat depths defined to ~150 m and ~37 m, respectively; species-specific paleotemperature equation for *N. dutertrei* from *Dekens et al.* [2002] (Mg/Ca = 0.6 · exp(0.08T)).

according to their Mg/Ca clearly reflects the expected depth habitats (Figure 3).

[24] As we are not able to establish core-top Mg/Ca versus temperature calibrations due to the restricted temperature range covered by our Caribbean samples, we compared our (dissolution-unaffected) core-top Mg/Ca data from <2000 m water depths to published Mg/Ca versus temperature relationships. Mg/Ca ratios of the deep-dwelling species

G. truncatulinoides dextral and sinistral, and *G. crassaformis* exhibit a clear relationship to temperature. Each species covers a regional temperature range of ~5–6°C when applying the habitat specification of *Schmuker and Schiebel* [2002] of ~160 m and ~230 m water depth, respectively (Figure 5a). The *G. truncatulinoides* dextral and sinistral, and *G. crassaformis* data fall onto published Mg/Ca versus temperature curves of *Anand et al.* [2003] proposed for multispecies planktonic foraminifers, and of *McKenna and Prell* [2004] for *G. truncatulinoides* dextral (Figure 5a). Also, the Mg/Ca data of Caribbean *G. sacculifer* agree with published calibration curves of *Nürnberg et al.* [1996a, 1996b], *Dekens et al.* [2002], and *Anand et al.* [2003] when relating water temperatures from ~40 m water depth [*Schmuker and Schiebel*, 2002] to the Mg/Ca ratios (Figure 5a).

[25] The Mg/Ca ratios of *G. tumida* are very close to those of *G. truncatulinoides* (Figure 4), suggesting akin living depths. If we assume a living depth of ~180 m, which is in accordance to *Ravelo and Fairbanks* [1992] and *Chaisson and Ravelo* [1997], than the according Mg/Ca versus temperature data fall onto the *Anand et al.* [2003] calibration curve (Figure 5b). Thermocline-dwelling *G. menardii* and *N. dutertrei* have less well-defined habitat specifications. In view of the low Mg/Ca ratios, the extremely shallow abundance maximum of ~40–50 m observed by *Schmuker and Schiebel* [2002] is highly unlikely to truly reflect the foraminiferal calcification depth (Figure 4). Assuming an average depth habitat of ~150 m water depth inferred from various sources [*Fairbanks et al.*, 1980, 1982; *Fairbanks and Wiebe*, 1980; *Sautter and Thunell*, 1991b; *Ravelo and Fairbanks*, 1992; *Chaisson and Ravelo*, 1997] results in Mg/Ca versus temperature data matching the *Anand et al.* [2003] calibration curve reasonably well (Figures 5c and 5d).

[26] In contrast to the above mentioned foraminiferal species, *G. ruber* is different. First, the spread of Mg/Ca ratios in dissolution-unaffected core-top samples is largest among our studied species. Second, Mg/Ca of *G. ruber* white and pink deviate from existing Mg/Ca versus temperature calibrations when considering depth habitats of ~34 m and ~37 m, respectively, which are the April-May abundance maxima in Caribbean plankton nets [*Schmuker and Schiebel*, 2002] (Figures 5c and 5d). Such depth estimates for *G. ruber* seem plausible as MOCNESS plankton tows from the western Gulf of Mexico show the depth preference

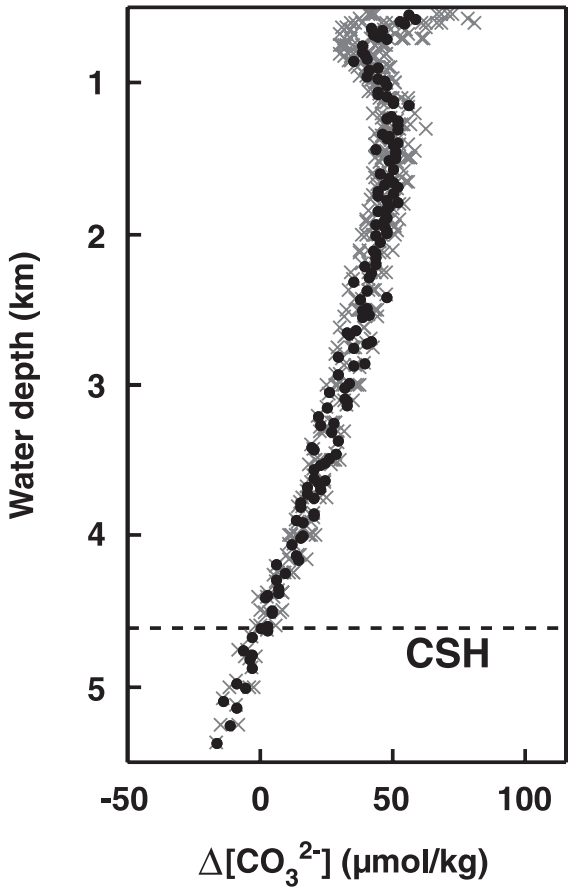

Figure 6. $\Delta[CO_3^{2-}]$, defined as the difference between the in situ carbonate ion concentration ($[CO_3^{2-}]$) and $[CO_3^{2-}]$ at saturation, versus water depth. Total alkalinity (TA) and TCO_2 data necessary to calculate the in situ $[CO_3^{2-}]$ were obtained from the World Ocean Circulation Experiment (WOCE) Line numbers A22 and A22_2003A (Caribbean stations 1–38 and 2–37, respectively; available at http://whpo.ucsd.edu/index.htm; Figure 1). The in situ $[CO_3^{2-}]$ was calculated using the program of *Lewis and Wallace* [1998] developed for CO_2 System Calculations. $[CO_3^{2-}]$ at saturation was calculated after *Jansen et al.* [2002]. Gray crosses mark computed $\Delta[CO_3^{2-}]$ data; black dots indicate $\Delta[CO_3^{2-}]$ data averaged for every 20 m water depth. CSH is calcite saturation horizon (dashed line) as the approximate top of the lysocline.

for *G. ruber* white to be 0–45 m, for *G. ruber* pink to be slightly deeper (25–65 m) [*Tedesco and Thunell*, 2003]. Even if one would assume a very shallow habitat of <10 m being ~0.2°C warmer than at ~30 m, the Mg/Ca data would still deviate from available calibration curves. The reason for that is not yet clear. It is evident, however, that *G. ruber* definitely occupies a shallower habitat than *G. sacculifer* as suggested by higher Mg/Ca (Figure 4) and generally lighter $\delta^{18}O$ values

Table 4. Species-Specific Parameters for Equations (2)–(7)[a]

Species	d Correction, Equation (6)				Δ Correction, Equation (7)			
	a	*b*	r^2	$d_{critical}$	*a*	*b*	r^2	$\Delta_{critical}$
G. crassaformis	6,833	1,962	0.61	2,838.4	−20.00	22.70	0.86	26.31
G. menardii	7,734	1,413	0.8	2,938.8	−27.61	15.03	0.78	22.88
G. ruber p.	9,403	1,381	0.79	2,631.1	−44.08	14.03	0.84	24.67
G. ruber w.	9,793	1,382	0.76	2,535.3	−40.93	12.61	0.71	25.28
G. sacculifer	12,030	2,088	0.75	2,967.8	−68.50	20.87	0.78	22.10
G. truncatulinoides d.	6,456	1,303	0.56	3,018.8	−16.23	13.79	0.74	20.17
G. truncatulinoides s.	7,471	1,888	0.65	2,746.4	−27.43	21.28	0.94	25.77
G. tumida	6,985	1,547	0.55	2,988.5	−6.62	9.43	0.32	17.70
N. dutertrei	7,057	1,484	0.67	2,567.9	−12.73	11.65	0.48	22.58

[a] Here, *a* are y axis intercepts; *b* is slope of the regression lines; r^2 are correlation coefficients; $d_{critical}$ (m) are species-specific water depths where Mg^{2+} removal starts; $\Delta_{critical}$ (μmol/kg) are species-specific $\Delta[CO_3^{2-}]$ levels where Mg^{2+} removal starts.

[*Anand et al.*, 2003]. Their oxygen isotope signal commonly points to summer sea-surface conditions [*Deuser*, 1987], and both *Flower et al.* [2004] and *Anand et al.* [2003] pointed out that Mg/Ca of *G. ruber* white commonly represents warmer than average temperatures in the Orca Basin (Gulf of Mexico) and in the Sargasso Sea, respectively.

4.4. Correcting Deep Water Mg/Ca Ratios for the Effect of Dissolution

[27] Dependent on the foraminiferal species and varieties, a major and systematic decrease in Mg/Ca ratios starts below species-specific critical water depths, which are situated in the depth interval between 2000–3000 m. This is far above the calcite saturation horizon (CSH) at ~4600 m (Figure 6), which approximates the present-day top of the lysocline at a $\Delta[CO_3^{2-}]$ (difference between the in situ carbonate ion concentration ($[CO_3^{2-}]$) and the $[CO_3^{2-}]$ at saturation) of 0 μmol/kg, and is equal to a calcite solubility ratio (Ω) of 1 [*Lewis and Wallace*, 1998; *Tyrrell and Zeebe*, 2004]. In fact, below >3000 m, Mg/Ca decreases linearly with increasing water depth (r^2 = 0.55–0.80; Figure 2; Table 4). This close relationship is also reflected in the linear decrease of Mg/Ca with decreasing $\Delta[CO_3^{2-}]$ (r^2 = 0.32–0.94; Figure 5; Table 4) below 20 μmol/kg (Figure 7; Table 4).

[28] As only few Mg/Ca ratios cover the interval between 2000–3000 m (40–20 μmol/kg $\Delta[CO_3^{2-}]$), the onset of dissolution was determined by calculating the intersection between the unaffected Mg/Ca means from <2000 m (>40 μmol/kg) and the regressions through the dissolution-affected ratios from >3000 m (<20 μmol/kg). The decrease of Mg/Ca can be described as

$$\Delta Mg/Ca = Mg/Ca_{initial} - Mg/Ca_{measured} \quad (1)$$

where ΔMg/Ca is the difference between the (unknown) initial, dissolution-unaffected Mg/Ca ($Mg/Ca_{initial}$) and the measured Mg/Ca ($Mg/Ca_{measured}$). A reasonable approximation for $Mg/Ca_{initial}$ is the mean Mg/Ca (Mg/Ca_{mean}) from <2000 m (Table 2). The intersection of the Mg/Ca_{mean} with the regression line calculated for Mg/Ca from >3000 m water depth and <20 μmol/kg $\Delta[CO_3^{2-}]$, respectively, provides the critical water depth ($d_{critical}$ in m) and the critical calcite saturation state ($\Delta_{critical}$ in μmol/kg), where Mg^{2+}-removal due to dissolution starts:

$$d_{critical} = a - b \cdot Mg/Ca_{mean} \quad (2)$$

$$\Delta_{critical} = a - b \cdot Mg/Ca_{mean} \quad (3)$$

where a is the y axis intercept, and b is the slope of the regression lines (Figures 2 and 7; Table 4). The levels of beginning preferential dissolution of Mg^{2+} appear to be species-specific. $\Delta_{critical}$ spans values of ~18–26 μmol/kg (Table 4) which correspond to Ω values of ~1.5, accompanied by $d_{critical}$ of ~2500–3000 m (Table 4).

[29] Different susceptibility of calcitic tests from different planktonic foraminiferal species to dissolution is a well-known feature [e.g., *Berger*, 1968, 1970, 1971], likewise is the heterogeneous distribution of Mg^{2+} in foraminiferal tests [*Bender et al.*, 1975; *Duckworth*, 1977; *Nürnberg*, 1995; *Brown and Elderfield*, 1996; *Nürnberg et al.*, 1996a; *Rosenthal et al.*, 2000; *Eggins et al.*, 2003; *McKenna and Prell*, 2004; *Anand and Elderfield*, 2005; *Bentov and Erez*, 2005, 2006]. *Sadekov et al.* [2005] recently illustrated by electron microprobe mapping that low-Mg/Ca (~1–5 mmol/mol) and high-Mg/Ca bands (~8–11 mmol/mol) alternate within tests of planktonic foraminifera. As Mg^{2+}

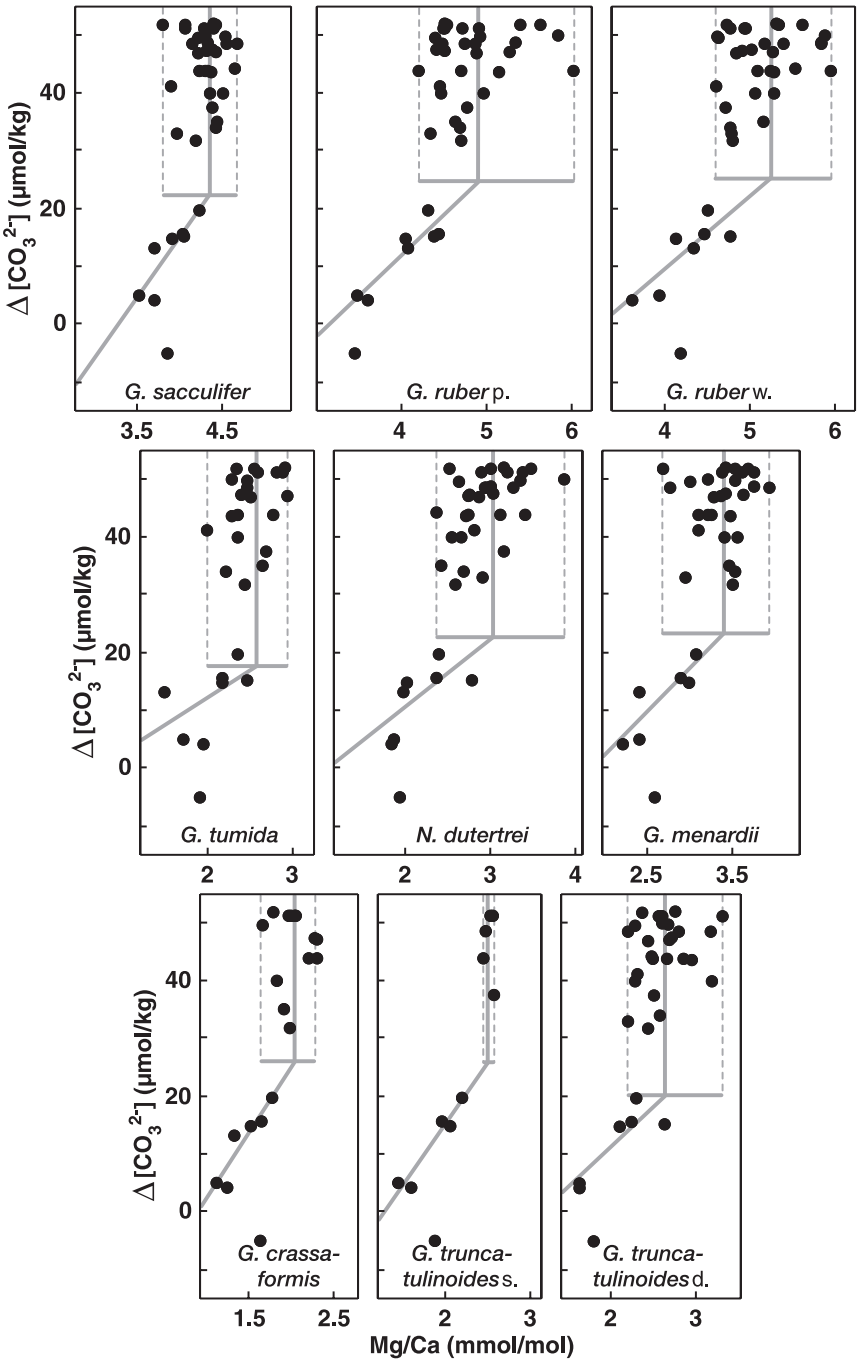

Figure 7. Mg/Ca ratios versus $\Delta[CO_3^{2-}]$ for each planktonic foraminiferal species and variety indicating significant Mg2+ loss below species-specific $\Delta[CO_3^{2-}]$ levels ($\Delta_{critical}$ = horizontal lines). $\Delta_{critical}$ is defined by the intercept between the vertical lines (species-specific mean Mg/Ca calculated from samples <2000 m water depth, similar to $\Delta[CO_3^{2-}] > 40$ µmol/kg (Table 2)) and diagonal lines (regression lines from Mg/Ca at $\Delta[CO_3^{2-}] < 20$ µmol/kg). Deepest core-top sample M35024–6 from below the CSH was defined as an outlier and excluded from the calculation of the regressions.

has a pronounced effect on the stability of biogenic calcite [*Walter and Morse*, 1985], and as ion activity products increase with increasing Mg^{2+}, *Brown and Elderfield* [1996] deduced that Mg-enriched phases are less dissolution resistant. The selective removal of Mg^{2+}-enriched foraminiferal parts with increasing dissolution should thus cause the reduction of the intraspecific Mg/Ca scatter, which is observed in samples from >3000 m water depth in comparison to shallow samples from

<2000 m. This reduction amounts to 36% for *G. ruber* white, 50% for *G. ruber* pink, 44% for *G. sacculifer*, 46% for *G. menardii*, 27% for *N. dutertrei*, 14% for *G. tumida*, 36% for *G. truncatulinoides* dextral, while *G. crassaformis* shows no discernable change.

[30] Nonetheless, the slopes b of the regression lines indicate a relatively uniform ~0.5–0.8 mmol/mol change in Mg/Ca ratios per kilometer water depth and ~0.04–0.11 mmol/mol per 1 μmol/kg decrease in $\Delta[CO_3^{2-}]$ with respect to Mg/Ca_{mean} for all studied foraminiferal species and varieties (Table 4). In contrast to observations of *Savin and Douglas* [1973], *Lorens et al.* [1977], *Brown and Elderfield* [1996], and *Rosenthal et al.* [2000], the relatively similar decline of Mg/Ca in combination with broadly the same $d_{critical}$ and $\Delta_{critical}$ (Figures 2 and 7; Table 4) for all foraminifers studied does not support the notion that calcite of shallow-dwelling foraminifers with higher Mg/Ca dissolves preferentially with respect to deep-dwelling species bearing lower Mg/Ca.

[31] The absolute change in Mg/Ca ratios of ~0.5–0.8 mmol/mol per kilometer water depth is equivalent to a relative decrease of ~11–29% per kilometer. Our results support previous core-top studies showing a decrease of Mg/Ca with increasing water depth [*Savin and Douglas*, 1973; *Bender et al.*, 1975; *Rosenthal and Boyle*, 1993]. For *G. sacculifer*, *Lorens et al.* [1977] showed a decrease in Mg/Ca of ~40% in tropical East Pacific Rise and central Pacific samples over a depth range from ~600–4000 m. Both *Lorens et al.* [1977] and *Brown and Elderfield* [1996] detected a decrease of 40% in Mg/Ca of *G. tumida* over a depth range from ~1900–4700 m, while the decline in Mg/Ca of *N. dutertrei* amounts to ~59% from ~600–3800 m, and ~25% for *G. ruber* from ~1900–4700 m [*Lorens et al.*, 1977], all from tropical Pacific samples. Assuming a linear Mg/Ca descent with depth, these numbers would convert to Mg/Ca reductions of ~12% for *G. sacculifer*, ~14% for *G. tumida*, ~18% for *N. dutertrei*, and ~9% for *G. ruber* per kilometer water depth. At Ontong Java Plateau, *Lea et al.* [2000] showed a decrease in Mg/Ca in tests of *G. ruber* by ~12% per kilometer water depth, while *Dekens et al.* [2002] revealed a decrease of ~14% per kilometer. At Sierra Leone Rise and Ceara Rise, a decrease in Mg/Ca of ~7% and ~5% per kilometer, respectively, was observed for *G. ruber* [*Dekens et al.*, 2002]. For *N. dutertrei*, *Dekens et al.* [2002] found a Mg/Ca decline of up to ~23% per kilometer.

[32] Our results on decreasing Mg/Ca ratios below species-specific $\Delta[CO_3^{2-}]$ levels of ~18–26 μmol/kg are in general accordance with *Dekens et al.* [2002], who also noted the onset of Mg^{2+} loss below ~20 μmol/kg $\Delta[CO_3^{2-}]$ at Ceara Rise (Atlantic) and Ontong Java Plateau (Pacific). In the South China Sea, *Whitko et al.* [2002] found declining Mg/Ca in core-top *G. ruber* below ~2000 m water depth, implying a strong dissolution effect below ~2000 m. This is considerably shallower than both, the present-day lysocline and the carbonate compensation depth in this ocean area at ~3000 m and ~3800 m, respectively [*Miao et al.*, 1994; *Feely et al.*, 2002, 2004]. Although we do not have $\Delta[CO_3^{2-}]$ values for this ocean basin at hand, we speculate that the onset of Mg/Ca change observed by *Whitko et al.* [2002] might coincide with the approximate threshold in $\Delta[CO_3^{2-}]$ of ~20 μmol/kg. It needs to be proven, though, whether this threshold is globally valid.

[33] In order to correct the measured Mg/Ca ratios for the selective loss of Mg^{2+} due to dissolution, ΔMg/Ca was calculated for every measured Mg/Ca from below $d_{critical}$ and $\Delta_{critical}$:

$$\Delta Mg/Ca = (d - d_{critical})/b \quad (4)$$

$$\Delta Mg/Ca = (\Delta_{critical} - \Delta)/b \quad (5)$$

where d is the water depth of the core-top sample in meter (with $d > d_{critical}$) (Tables 1 and 2), and Δ is the averaged $\Delta[CO_3^{2-}]$ in μmol/kg at the seafloor (with $\Delta < \Delta_{critical}$) (Figure 6). We then combined equations (1) and (4), as well as (1) and (5) to recalculate the dissolution-unaffected $Mg/Ca_{initial}$ (water depth correction (d-corrected) according to equation (4) (Figure 8); and $\Delta_{critical}$ correction (Δ-corrected) according to equation (5)):

$$Mg/Ca_{initial}(d - corrected) = Mg/Ca_{measured} + (d - d_{critical})/b \quad (6)$$

$$Mg/Ca_{initial}(\Delta - corrected) = Mg/Ca_{measured} + (\Delta_{critical} - \Delta)/b \quad (7)$$

[34] Both independently developed routines for the correction of dissolution-induced Mg/Ca decline produce comparable results indicating that selective Mg^{2+} removal is mainly driven by the calcite saturation state (Figure 9). Application of the correction routines reduces the overall intraspecific variability of Mg/Ca by ~24–64% (Figure 8).

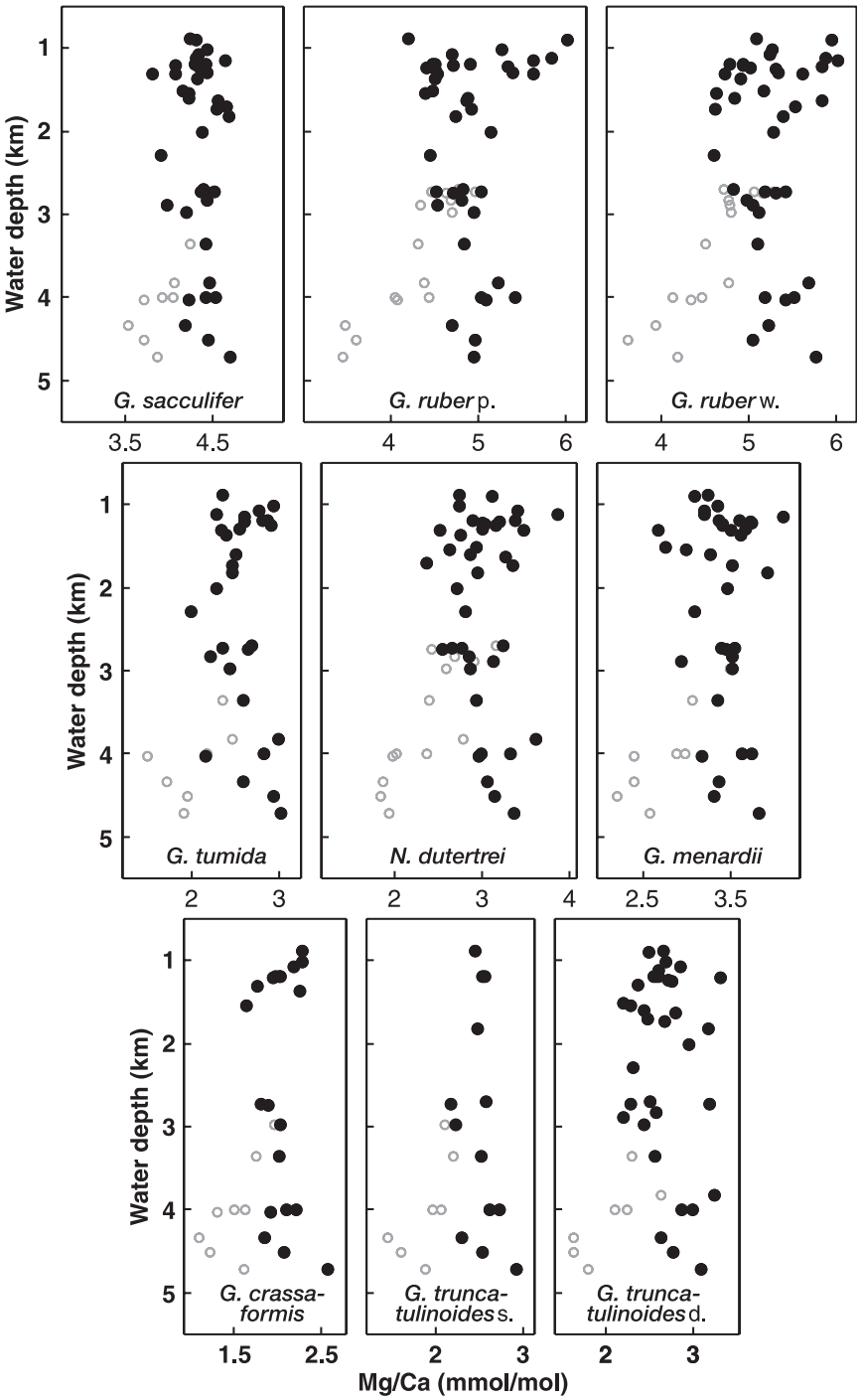

Figure 8. Foraminiferal Mg/Ca ratios versus water depth (black dots): Mg/Ca from below $d_{critical}$ were corrected for water-depth induced calcite dissolution according to equation (6). For comparison, the measured, noncorrected Mg/Ca data are included (circles). The application of the correction routine leads to a reduction of the intraspecific Mg/Ca variability by 24–64%.

4.5. Implications for Paleorecords

[35] We chose the Mg/Ca records of *G. ruber* white of two Caribbean cores [*Schmidt et al.*, 2004] to test the downcore applicability of the proposed correction routine. Today, both records chart similar temperature conditions within the Columbian Basin (Figure 1) and hence are expected to show similar Mg/Ca ratios. The impact of dissolution on the Holocene (3–6 kyrs) mean Mg/Ca from shal-

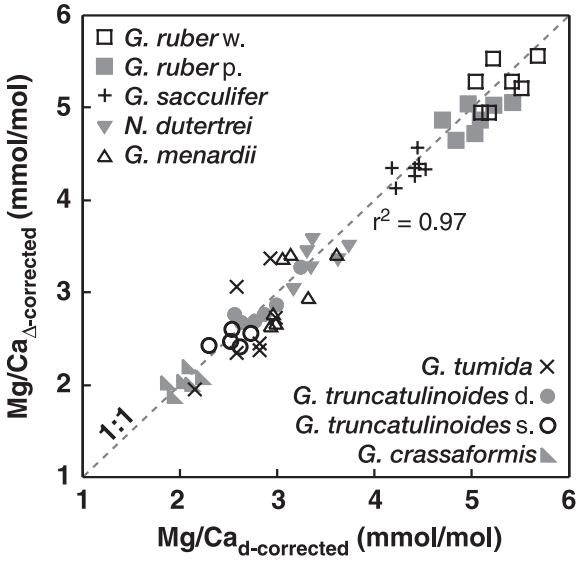

Figure 9. Depth-corrected (d-corrected, equation (6)) versus $\Delta[CO_3^{2-}]$-corrected (Δ-corrected, equation (7)) Mg/Ca ratios: The independently corrected ratios from below $d_{critical}$ and $\Delta_{critical}$ highly correlate ($r^2 = 0.97$). Related high probability values ($p = 0.77$) imply that the corrected Mg/Ca means of all species and varieties do not statistically deviate from each other, implying that the selective removal of Mg^{2+} from foraminiferal calcite is mainly a function of the calcite saturation state $\Delta[CO_3^{2-}]$.

lower ODP Site 999A (2827 m, 4.13 mmol/mol) appears to be less than on Mg/Ca from deeper site VM22–128 (3623 m, 3.75 mmol/mol), differing by 0.38 mmol/mol. Depth correction (equation (6); parameters see Table 4) leads to higher Holocene Mg/Ca of 4.34 mmol/mol at ODP Site 999A and 4.53 mmol/mol at site VM28–122, reducing the offset to 0.19 mmol/mol. Such inter-site offset converts to a ~0.5°C difference (calculated after *Anand et al.* [2003]; see Table 2), which is in accordance with the modern temperature pattern in the Columbian Basin.

[36] For glacial times, instead, reduced pCO_2 and increased $[CO_3^{2-}]$ in Caribbean intermediate and deep waters [*Barker and Elderfield*, 2002; *Broecker and Clark*, 2002] suggest a better carbonate preservation [*Haddad and Droxler*, 1996; *Anderson and Archer*, 2002]. Hence Mg/Ca ratios should have been unaffected by dissolution effects even at greater water depths. This is reflected in the similar last glacial (19–21 kyrs) mean Mg/Ca of Caribbean cores ODP 999A and VM28–122 [*Schmidt et al.*, 2004], both revealing 3.36 mmol/mol.

5. Conclusions

[37] We analyzed Mg/Ca ratios in tests of seven planktonic foraminiferal species and four of their varieties from 42 Caribbean and tropical Atlantic core-top samples covering water depths of ~900–4700 m in order to quantify the effect of dissolution on Mg/Ca. As lateral temperature gradients at similar water depths in the study area are minor, the well-known temperature effect on intraspecific Mg/Ca variations is considered to be minimal. Shallow core-top samples from above 2000 m water depth being unaffected by dissolution processes, clearly reveal interspecific differences in Mg/Ca with high ratios in shallow-dwelling, and low ratios in deep-dwelling species. This pattern reflects the expected habitat depths, and clearly points to different calcification depths at different temperature regimes.

[38] The core-top samples exhibit a linear decline of foraminiferal Mg/Ca ratios below water depths of ~2500–3000 m ($d_{critical}$) depending on the foraminiferal species or variety. Hence the onset of selective Mg^{2+} removal ($d_{critical}$) takes place far above the present-day lysocline and concurs with calcite saturation state $\Delta[CO_3^{2-}]$ levels of ~18–26 μmol/kg ($\Delta_{critical}$). Mg/Ca from above these species-specific critical levels appear to remain stable and hence are considered to be unaffected by dissolution. Nonetheless, the intraspecific variability at shallow depths is larger than at greater water depths.

[39] Below the species-specific levels ($\Delta_{critical}$ and $d_{critical}$) of apparent Mg^{2+} removal, Mg/Ca ratios decline linearly by ~0.04–0.11 mmol/mol per 1 mol/kg decrease in $\Delta[CO_3^{2-}]$ and ~0.5–0.8 mmol/mol per kilometer water depth. The relatively similar rates of Mg/Ca change, and the broadly similar dcritical and $\Delta_{critical}$ for all species and varieties studied, imply that low magnesium calcite of shallow-dwelling foraminifers showing higher Mg/Ca does not dissolve preferentially with respect to calcite of deep-dwelling species bearing lower Mg/Ca.

[40] We developed independent routines to correct core-top Mg/Ca ratios from below $\Delta_{critical}$ and $d_{critical}$ for the effect of dissolution. Both routines produce comparable results, implying that the selective Mg^{2+} removal is mainly driven by the calcite saturation state at the seafloor. They may be used as robust approaches for the assessment and

correction of the dissolution effect on planktonic Mg/Ca. The water-depth correction of Mg/Ca (equation (6)), however, should only be applied to samples from ocean areas with resembling calcite saturation states. Instead, the $\Delta[CO_3^{2-}]$ correction (equation (7)) is applicable to any ocean area as long as the $\Delta[CO_3^{2-}]$ levels are known. The critical $\Delta[CO_3^{2-}]$ level of ~20 μmol/kg as an effective threshold for the onset of Mg^{2+} removal from low magnesium foraminiferal calcite may be globally valid in this respect, even through geological time spans. The correction routines proposed here may help to improve core-top Mg/Ca versus temperature calibrations, and to recalculate initial Holocene Mg/Ca, from which paleotemperature estimates can be derived.

Acknowledgments

[41] This study was funded by the German Ministry of Education and Research (BMBF) under project 03G0164 and the Leibniz Award Du 129/33. KIA-AMS^{14}C analyses were performed at the Leibniz-Labor for Radiometric Dating and Isotope Research, Kiel, Germany. We thank Silvia Koch, Karin Kiling, Daniel Oesterwind, and Stefan Dennenmoser for technical support and laboratory assistance and Anke Schneider and Douglas W. R. Wallace for assistance with the running of the co2sys program. We are grateful for the useful comments of Joachim Schönfeld, Martin Ziegler, and the reviewers Robert C. Thunell and Luke C. Skinner, who considerably improved the manuscript.

References

Anand, P., and H. Elderfield (2005), Variability of Mg/Ca and Sr/Ca between and within the planktonic foraminifers *Globigerina bulloides* and *Globorotalia truncatulinoides*, *Geochem. Geophys. Geosyst.*, *6*, Q11D15, doi:10.1029/2004GC000811.

Anand, P., H. Elderfield, and M. H. Conte (2003), Calibration of Mg/Ca thermometry in planktonic foraminifera from a sediment trap time series, *Paleoceanography*, *18*(2), 1050, doi:10.1029/2002PA000846.

Anderson, D. M., and D. Archer (2002), Glacial-interglacial stability of ocean pH inferred from foraminifer dissolution rates, *Nature*, *416*, 70–73.

Barker, S., and H. Elderfield (2002), Foraminiferal calcification response to glacial-interglacial changes in atmospheric CO_2, *Science*, *297*, 833–836.

Barker, S., M. Greaves, and H. Elderfield (2003), A study of cleaning procedures used for foraminiferal Mg/Ca paleothermometry, *Geochem. Geophys. Geosyst.*, *4*(9), 8407, doi:10.1029/2003GC000559.

Bé, A. W. H. (1977), An ecological, zoogeographic and taxonomic review of recent planktonic foraminifera, in *Oceanic Micropaleontology*, vol. 1, edited by A. T. S. Ramsay, pp. 1–100, Elsevier, New York.

Bé, A. W. H. (1980), Gametogenic calcification in a spinose planktonic foraminifer *Globigerinoides sacculifer* (Brady), *Mar. Micropaleontol.*, *5*, 283–310.

Bé, A. W. H., and D. B. Ericson (1963), Aspects of calcification in planktonic foraminifera, *Ann. N. Y. Acad. Sci.*, *109*, 65–81.

Bé, A. W. H., and L. Lott (1964), Shell growth and structure of planktonic foraminifera, *Science*, *145*, 823–824.

Bé, A. W. H., O. R. Anderson, W. W. J. Faber, and D. A. Caron (1983), Sequence of morphological and cytoplasmic changes during gametogenesis in the planktonic foraminifera *Globigerinoides sacculifer* (Brady), *Micropaleontology*, *29*, 310–325.

Bender, M. L., R. B. Lorens, and F. D. Williams (1975), Sodium, magnesium and strontium in the tests of planktonic foraminifera, *Micropaleontology*, *21*, 448–459.

Bentov, S., and J. Erez (2005), Novel oberservations on biomineralization processes in foraminifera and implications for Mg/Ca ratio in the shells, *Geology*, *33*(11), 841–844, doi:10.1130/G21800.1.

Bentov, S., and J. Erez (2006), Impact of biomineralization processes on the Mg content of foraminiferal shells: A biological perspective, *Geochem. Geophys. Geosyst.*, *7*, Q01P08, doi:10.1029/2005GC001015.

Berger, W. H. (1968), Planktonic foraminifera: Selective solution and paleoclimate interpretation, *Deep Sea Res. Oceanogr. Res.*, *15*, 31–43.

Berger, W. H. (1970), Planktonic foraminifera: Selective solution and the lysocline, *Mar. Geol.*, *8*, 111–138.

Berger, W. H. (1971), Sedimentation of planktonic foraminifera, *Mar. Geol.*, *11*, 325–358.

Bijma, J., J. Erez, and C. Hemleben (1990), Lunar and semilunar reproductive cycles in some spinose planktonic foraminifers, *J. Foraminiferal Res.*, *20*(2), 117–127.

Bijma, J., C. Hemleben, and K. Wellnitz (1994), Population dynamics of the planktic foraminifer *Globigerinoides sacculifer* (Brady) from the central Red Sea, *Deep Sea Res., Part I*, *41*(3), 485–510.

Broecker, W. S., and E. Clark (2002), Carbonate ion concentration in glacial-age deep waters of the Caribbean Sea, *Geochem. Geophys. Geosyst.*, *3*(3), 1021, doi:10.1029/2001GC000231.

Brown, K., and K. Azmy (2005), Morphological and geochemical analysis of recent Caribbean Globorotaliid foraminifera, in *Geophys. Res. Abstr.*, *7*, sRef-ID:1607-7962/gra/EGU05-A-05254.

Brown, S. J., and H. Elderfield (1996), Variations in Mg/Ca and Sr/Ca ratios of planktonic foraminifera caused by post-depositional dissolution: Evidence of shallow Mg-dependent dissolution, *Paleoceanography*, *11*(5), 543–551.

Bulgakov, N. P., and O. D. Lomakin (1995), Local sound channels in the Caribbean Sea, *Oceanology*, *34*(6), 744–749.

Chaisson, W. P., and A. C. Ravelo (1997), Changes in upper water-column structure at Site 925, Late Miocene-Pleistocene: Planktonic foraminifer assemblage and isotopic evidence, *Proc. Ocean Drill. Program Sci. Results*, *154*, 255–268.

Corredor, J. E., and J. M. Morell (2001), Seasonal variation of physical and biogeochemical features in eastern Caribbean Surface Water, *J. Geophys. Res.*, *106*(C3), 4517–4525.

Cronblad, H. G., and B. A. Malmgren (1981), Climatically controlled variation of Sr and Mg in Quaternary planktic foraminifera, *Nature*, *291*, 61–64.

Curry, W. B., and T. J. Crowley (1987), The ^{13}C of equatorial Atlantic surface waters: Implications for the ice age pCO_2 levels, *Paleoceanography*, *2*(5), 489–517.

Curry, W. B., R. C. Thunell, and S. Honjo (1983), Seasonal changes in the isotopic composition of planktonic foramini-

fera collected in Panama Basin sediment traps, *Earth Planet. Sci. Lett.*, *64*, 33–43.

de Villiers, S. (2003), Dissolution effects on foraminiferal Mg/Ca records of sea surface temperature in the western equatorial Pacific, *Paleoceanography*, *18*(3), 1070, doi:10.1029/2002PA000802.

Dekens, P. S., D. W. Lea, D. K. Pak, and H. J. Spero (2002), Core top calibration of Mg/Ca in tropical foraminifera: Refining paleotemperature estimation, *Geochem. Geophys. Geosyst.*, *3*(4), 1022, doi:10.1029/2001GC000200.

Deuser, W. G. (1987), Seasonal variations in isotopic composition and deep-water fluxes of the tests of perennially abundant planktonic foraminifera of the Sargasso Sea: Results from sediment trap collections and their paleoceanographic significance, *J. Foraminiferal Res.*, *17*, 14–27.

Deuser, W. G., and E. H. Ross (1989), Seasonally abundant planktonic foraminifera of the Sargasso Sea: Succession, deep-water fluxes, isotopic compositions, and paleoceanographic implications, *J. Foraminiferal Res.*, *19*, 268–293.

Duckworth, D. L. (1977), Magnesium concentrations in the tests of the planktonic foraminifer *Globorotalia truncatulinoides*, *J. Foraminiferal Res.*, *4*, 304–312.

Duplessy, J. C., P. L. Blanc, and A. W. H. Bé (1981), Oxygen-18 enrichment of planktic foraminifera due to gametogenic calcification below the euphotic zone, *Science*, *213*, 1247–1249.

Eggins, S., P. DeDeckker, and J. Marshall (2003), Mg/Ca variation in planktonic foraminifera tests: Implications for reconstructing palaeo-seawater temperature and habitat migration, *Earth Planet. Sci. Lett.*, *212*, 291–306.

Elderfield, H., and G. Ganssen (2000), Past temperature and $\delta^{18}O$ of surface ocean waters inferred from foraminiferal Mg/Ca ratios, *Nature*, *405*, 442–445.

Elderfield, H., M. Vautravers, and M. Cooper (2002), The relationship between shell size and Mg/Ca, Sr/Ca, $\delta^{18}O$, and $\delta^{13}C$ of species of planktonic foraminifera, *Geochem. Geophys. Geosyst.*, *3*(8), 1052, doi:10.1029/2001GC000194.

Erez, J., and S. Honjo (1981), Comparison of isotopic composition of planktonic foraminifera in plankton tows, sediment traps and sediments, *Palaeogeogr. Palaeoclimatol. Palaeoecol.*, *33*, 129–156.

Fairbanks, R. G., and P. H. Wiebe (1980), Foraminifera and chlorophyll maximum — Vertical distribution, seasonal succession and paleoceanographic significance, *Science*, *209*, 1524–1526.

Fairbanks, R. G., P. H. Wiebe, and A. W. H. Bé (1980), Vertical distribution and isotopic composition of living planktonic foraminifera in the western North Atlantic, *Science*, *207*, 61–63.

Fairbanks, R. G., M. Sverdlove, R. Free, P. H. Wiebe, and A. W. H. Bé (1982), Vertical distribution and isotopic fractionation of living planktonic foraminifera from the Panama Basin, *Nature*, *298*, 841–844.

Feely, R. A., et al. (2002), In situ calcium carbonate dissolution in the Pacific Ocean, *Global Biogeochem. Cycles*, *16*(4), 1144, doi:10.1029/2002GB001866.

Feely, R. A., C. L. Sabine, K. Lee, W. Berelson, J. Kleypas, V. J. Fabry, and F. J. Millero (2004), Impact of anthropogenic CO_2 on the $CaCO_3$ system in the oceans, *Science*, *305*, 362–366.

Flower, B. P., D. W. Hastings, H. W. Hill, and T. M. Quinn (2004), Phasing of deglacial warming and Laurentide Ice Sheet meltwater in the Gulf of Mexico, *Geology*, *32*(7), 597–600.

Fratantoni, D. M., R. J. Zantopp, W. E. Johns, and J. L. Miller (1997), Updated bathymetry of the Anageda-Jungfern Passage complex and implications for Atlantic inflow to the abyssal Caribbean Sea, *J. Mar. Res.*, *55*, 847–860.

Ganssen, G., and D. Kroon (2000), The isotopic signature of planktonic foraminifera from NE-Atlantic surface sediments: Implications for the reconstruction of past oceanic conditions, *J. Geol. Soc. London*, *157*, 693–699.

Haddad, G. A., and A. W. Droxler (1996), Metastable $CaCO_3$ dissolution at intermediate water depths of the Caribbean and western North Atlantic: Implications form intermediate water circulation during the past 200,000 years, *Paleoceanography*, *11*(6), 701–716.

Hastings, D. W., S. R. Emerson, J. Erez, and B. R. Nelson (1996), Vanadium in foraminiferal calcite: Evaluation of a method to determine paleo-seawater vanadium concentrations, *Geochim. Cosmochim. Acta*, *60*(19), 3701–3715.

Hastings, D. W., S. R. Emerson, J. Erez, and B. R. Nelson (1998), Foraminiferal magnesium in *Globigerinoides sacculifer* as a paleotemperature proxy, *Paleoceanography*, *13*(2), 161–169.

Hecht, A. D., E. V. Eslinger, and L. B. Garmon (1975), Experimental studies on the dissolution of planktonic foraminifera, in *Dissolution of Deep-Sea Carbonates, Spec. Publ. 13*, edited by W. V. Sliter, A. W. H. Bé, and W. H. Berger, pp. 56–69, Cushman Found. for Foraminiferal Res., Washington, D. C.

Hemleben, C., M. Spindler, and O. R. Anderson (Eds.) (1989), *Modern Planktonic Foraminifera*, 363 pp., Springer, New York.

Hilbrecht, H., (Ed.) (1996), *Extant Planktic Foraminifera and the Physical Environment in the Atlantic and Indian Oceans, Neue Folge 300*, 93 pp., Mitteilungen aus dem Geologischen Institut der Eidgen, Tech. Hochschule und der Univ. Zürich, Zurich, Switzerland.

Jansen, H., R. E. Zeebe, and D. A. Wolf-Gladrow (2002), Modeling the dissolution of settling $CaCO_3$ in the ocean, *Global Biogeochem. Cycles*, *16*(2), 1027, doi:10.1029/2000GB001279.

Johns, W. E., T. L. Townsend, D. M. Fratantoni, and W. D. Wilson (2002), On the Atlantic inflow to the Caribbean Sea, *Deep Sea Res., Part I*, *49*, 211–243.

Joyce, T. M., R. S. Pickart, and R. C. Millard (1999), Long-term hydrographic changes at 52 and 66°W in the North Atlantic Subtropical Gyre and Caribbean, *Deep Sea Res., Part II*, *46*, 245–278.

Kameo, K. (2002), Late Pliocene Caribbean surface water dynamics and climatic changes based on calcareous nannofossil records, *Palaeogeogr. Palaeoclimatol. Palaeoecol.*, *179*, 211–226.

Kemle-von Mücke, S., and H. Oberhänsli (1999), The distribution of living planktic foraminifera in relation to southeast Atlantic oceanography, in *Use of Proxies in Paleoceanography: Examples from the South Atlantic*, edited by G. Fischer and G. Wefer, pp. 91–115, Springer, New York.

Kennett, J. P., and M. S. Srinivasan (Eds.) (1983), *Neogene Planktonic Foraminifera, A Phylogenetic Atlas*, 265 pp., John Wiley, Hoboken, N. J.

Kroon, D., and K. Darling (1995), Size and upwelling control of the stable isotope composition of *Neogloboquadrina dutertrei* (d'Orbigny), *Globigerinoides ruber* (d'Orbigny), and *Globigerina bulliodes* (d'Orbigny): Examples from the Panama Basin and the Arabian Sea, *J. Foraminiferal Res.*, *25*, 39–52.

Larsen, J. C. (1992), Transport and heat flux of the Florida Current at 27°N derived from the cross-steam voltages and profiling data: Theory and observation, *Philos. Trans. R. Soc. London, Ser. A*, *338*, 169–236.

Lea, D. W. (2003), Elemental and isotopic proxies of past ocean temperatures, in *Treatise on Geochemistry: The Oceans and Marine Geochemistry*, vol. 6, edited by H. Elderfield, pp. 365–390, Elsevier, New York.

Lea, D. W., T. A. Mashiotta, and H. J. Spero (1999), Controls on the magnesium and strontium uptake in planktonic foraminifera determined by live culturing, *Geochim. Cosmochim. Acta*, *63*(16), 2369–2379.

Lea, D. W., D. K. Pak, and H. J. Spero (2000), Climate impact of late quaternary equatorial Pacific sea surface temperature variations, *Science*, *289*, 1719–1724.

Lewis, E., and D. W. R. Wallace (Eds.) (1998), *co2sys — Program Developed for CO_2System Calculations, oRNL/CDIAC-105*, Carbon Dioxide Inf. Anal. Cent., Oak Ridge Natl. Lab., U.S. Dep. of Energy, Oak Ridge, Tenn.

Lin, H., L. C. Peterson, J. T. Overpeck, S. E. Trumbore, and D. W. Murray (1997), Late Quaternary climate change from $\delta^{18}O$ records of multiple species of planktonic foraminifera: High-resolution records from the anoxic Cariaco Basin, Venezuela, *Paleoceanography*, *12*(3), 415–427.

Lohmann, G. (1995), A model for variation in the chemistry of planktonic foraminifera due to secondary calcification and selective dissolution, *Paleoceanography*, *10*(3), 445–457.

Lorens, R. B., D. F. Williams, and M. L. Bender (1977), The early nonstructual chemical diagenesis of foraminiferal calcite, *J. Sediment. Petrol.*, *47*, 1602–1609.

Mashiotta, T. A., D. W. Lea, and H. J. Spero (1999), Glacial-interglacial changes in Subantarctic sea surface temperature and $\delta^{18}O$-water using foraminiferal Mg, *Earth Planet. Sci. Lett.*, *170*, 417–432.

McConnell, M. C., and R. C. Thunell (2005), Calibration of the planktonic foraminiferal Mg/Ca paleothermometer: Sediment trap results from the Guaymas Basin, Gulf of California, *Paleoceanography*, *20*, PA2016, doi:10.1029/2004PA001077.

McKenna, V. S., and W. L. Prell (2004), Calibration of the Mg/Ca of *Globorotalia truncatulinoides* (R) for the reconstruction of marine temperature gradients, *Paleoceanography*, *19*, PA2006, doi:10.1029/2000PA000604.

Miao, Q., R. C. Thunell, and D. M. Anderson (1994), Glacial-Holocene carbonate dissolution and sea surface in the South China and Sulu seas, *Paleoceanography*, *9*(2), 269–290.

Molinari, R., E. Johns, and J. F. Festa (1990), The annual cycle of meridional heat flux in the Atlantic Ocean at 26.5°N, *J. Phys. Oceanogr.*, *20*, 476–482.

Morrison, J. M., and W. D. Nowlin (1982), General distribution of water masses within the Eastern Caribbean Sea during the winter of 1972 and fall of 1973, *J. Geophys. Res.*, *87*(C6), 4207–4229.

Morrison, J. M., and O. P. Smith (1990), Geostrophic transport variability along the Aves Ridge in the eastern Caribbean Sea during 1985 and 1986, *J. Geophys. Res.*, *95*, 699–710.

Mulitza, S., A. Dürkoop, W. Hale, and G. Wefer (1997), Planktonic foraminifera as recorders of past surface-water stratification, *Geology*, *25*(4), 335–338.

Mulitza, S., B. Donner, G. Fischer, A. Paul, J. Pätzold, C. Rühlemann, and M. Segl (2003), The South Atlantic oxygen isotope record of planktic foraminifera, in *The South Atlantic in the Late Quaternary: Reconstruction of Material Budgets and Current Systems*, edited by G. Wefer, S. Mulitza, and V. Ratmeyer, pp. 121–142, Springer, New York.

National Oceanographic and Data Center (NODC) (2001), *World Ocean Atlas 2001: Objective Analyses, Data Statistics, and Figures*, CD-ROM documentation, Natl. Oceanic and Atmos. Admin., Silver Spring, Md.

Nürnberg, D. (1995), Magnesium in tests of *Neogloboquadrina pachyderma* sinistral from high Northern and Southern latitudes, *J. Foraminiferal Res.*, *25*(4), 350–368.

Nürnberg, D. (2000), Taking the temperature of past ocean surfaces, *Science*, *289*, 1698–1699.

Nürnberg, D., and J. Groeneveld (2006), Pleistocene variability of the Subtropical Convergence at East Tasman Plateau: Evidence from planktonic foraminiferal Mg/Ca (ODP Site 1172A), *Geochem. Geophys. Geosyst.*, *7*, Q04P11, doi:10.1029/2005GC000984.

Nürnberg, D., J. Bijma, and C. Hemleben (1996a), Assessing the reliability of magnesium in foraminiferal calcite as a proxy for water mass temperatures, *Geochim. Cosmochim. Acta*, *60*(5), 803–814.

Nürnberg, D., J. Bijma, and C. Hemleben (1996b), Erratum, *Geochim. Cosmochim. Acta*, *60*(13), 2483–2484.

Nürnberg, D., A. Müller, and R. R. Schneider (2000), Paleo-sea surface temperature calculations in the equatorial East Atlantic from Mg/Ca ratios in planktic foraminifera: A comparison to sea surface temperature estimates from Uk'37 oxygen isotopes, and foraminiferal transfer function, *Paleoceanography*, *15*(1), 124–134.

Nürnberg, D., J. Schönfeld, W.-C. Dullo, and C. Rühlemann (Eds.) (2003), *RV SONNE: Cruise Report SO164 RASTA (2002)*, vol. 109, 151 pp., GEOMAR Report, IFM-GEOMAR, Kiel, Germany.

Ortiz, J. D., A. C. Mix, and R. W. Collier (1995), Environmental control of living symbiotic and asymbiotic foraminifera of the California Current, *Paleoceanography*, *10*, 987–1009.

Ortiz, J. D., A. C. Mix, W. Rugh, J. M. Watkins, and R. W. Collier (1996), Deep-dwelling planktonic foraminifera of the Northeast Pacific reveal environmental control of oxygen and carbon isotopic disequilibria, *Geochim. Cosmochim. Acta*, *60*, 4509–4523.

Ortiz, J. D., A. C. Mix, S. Hostetler, and M. Kashgarian (1997), The California Current of the Last Glacial Maximum at 42°N: Reconstruction based on multiple proxies, *Paleoceanography*, *12*, 191–206.

Pahnke, K., and R. Zahn (2005), Southern Hemisphere water mass conversion linked with North Atlantic climate variability, *Science*, *18*, 1741–1746.

Ravelo, A. C., and R. G. Fairbanks (1992), Oxygen isotopic composition of multiple species of planktonic foraminifera: Recorders of the modern photic zone temperature gradient, *Paleoceanography*, *7*(6), 815–831.

Reimer, P. J., et al. (2004), IntCal04 Terrestrial radiocarbon age calibration, 26–0 ka BP, *Radiocarbon*, *46*, 1029–1058.

Rickaby, R., and P. Halloran (2005), Cool La Niña during the warmth of the Pliocene?, *Science*, *307*, 1948–1952, doi:10.1126/science.1104666.

Rosenthal, Y., and E. A. Boyle (1993), Factors controlling the flouride content of planktonic foraminifera: An evaluation of its paleoceanographic applicability, *Geochim. Cosmochim. Acta*, *57*, 335–346.

Rosenthal, Y., and G. P. Lohmann (2002), Accurate estimation of sea surface temperatures using dissolution-corrected calibrations for Mg/Ca paleothermometry, *Paleoceanography*, *17*(3), 1044, doi:10.1029/2001PA000749.

Rosenthal, Y., G. P. Lohmann, K. C. Lohmann, and R. M. Sherrell (2000), Incorporation and preservation of Mg in *Globigerinoides sacculifer*: Implications for reconstructing the temperature and $^{18}O/^{16}O$ of seawater, *Paleoceanography*, *15*(1), 135–145.

Rosenthal, Y., et al. (2004), Interlaboratory comparison study of Mg/Ca and Sr/Ca measurements in planktonic foramini-

fera for paleoceanographic research, *Geochem. Geophys. Geosyst.*, *5*, Q04D09, doi:10.1029/2003GC000650.

Russell, A. D., S. Emerson, B. K. Nelson, J. Erez, and D. W. Lea (1994), Uranium in foraminiferal calcite as a recorder of seawater uranium concentrations, *Geochim. Cosmochim. Acta*, *58*, 671–681.

Russell, A. D., B. Hönisch, H. J. Spero, and D. W. Lea (2004), Effects of seawater carbonate ion concentration and temperature on shell U, Mg, and Sr in cultured planktonic foraminifera, *Geochim. Cosmochim. Acta*, *68*(21), 4347–4361, doi:10.1016/j.gca.2004.03.013.

Sadekov, A. Yu., S. M. Eggins, and P. De Deckker (2005), Characterization of Mg/Ca distributions in planktonic foraminifera species by electron microprobe mapping, *Geochem. Geophys. Geosyst.*, *6*, Q12P06, doi:10.1029/2005GC000973.

Sautter, L. R., and R. C. Thunell (1991a), Seasonal variability in the oxygen and carbon isotopic composition of planktonic foraminifera from an upwelling environment: Sediment trap results from the San Pedro Basin, Southern California Bight, *Paleoceanography*, *6*, 307–334.

Sautter, L. R., and R. C. Thunell (1991b), Planktonic foraminiferal response to upwelling and seasonal hydrographic conditions: Sediment trap results from the San Pedro Basin, Southern California Bight, *J. Foraminiferal Res.*, *21*, 347–363.

Savin, S. M., and R. G. Douglas (1973), Stable isotope and magnesium geochemistry of recent planktonic foraminifera from the South Pacific, *Geol. Soc. Am. Bull.*, *84*(7), 2327–2342.

Schlitzer, R. (Ed.) (2002), *Ocean Data View*, Alfred Wegener Inst., Bremerhaven, Germany. (Available at http://www.awi-bremerhaven.de/GEO/ODV.)

Schmidt, M. W., H. J. Spero, and D. W. Lea (2004), Links between salinity variation in the Caribbean and North Atlantic thermohaline circulation, *Nature*, *428*, 160–163.

Schmuker, B. (2000), Recent planktic foraminifera in the Caribbean Sea: Distribution, ecology and taphonomy, Ph.D. thesis, ETH Zürich, Zurich, Switzerland.

Schmuker, B., and R. Schiebel (2002), Planktic foraminifers and hydrography of the eastern and northern Caribbean Sea, *Mar. Micropaleontol.*, *428*, 387–403.

Schott, F. A., T. N. Lee, and R. Zantopp (1988), Variability of structure and transport of the Florida Current in the period range of days to seasonal, *J. Phys. Oceanogr.*, *18*(9), 1209–1230.

Schweitzer, P. N., and G. P. Lohmann (1991), Ontogeny and habitat of modern menardiiform planktonic foraminifera, *J. Foraminiferal Res.*, *21*, 332–346.

Spero, H. J., and D. F. Williams (1989), Opening the carbon isotope vital effect black box, 1, Seasonal temperatures in the euphotic zone, *Paleoceanography*, *4*(6), 593–601.

Stalcup, M. C., W. G. Metcalf, and R. G. Johnson (1975), Deep Caribbean inflow through the Anageda-Jungfern Passage, *J. Mar. Res.*, *33*, suppl., 15–35.

Steinke, S., H. Chiu, P. Yu, C. Shen, L. Löwemark, H. Mii, and M. Chen (2005), Mg/Ca ratios of two *Globigerinoides ruber* (white) morphotypes: Implications for reconstructing past tropical/subtropical surface water conditions, *Geochem. Geophys. Geosyst.*, *6*, Q11005, doi:10.1029/2005GC000926.

Stuiver, M., P. J. Reimer, and R. W. Reimer (Eds.) (2005), CALIB Radiocarbon Calibration, version CALIB 5.0.2html, ^{14}CHRONO Centre, Queens Univ. Belfast, Belfast, UK. (Available at http://radiocarbon.pa.qub.ac.uk/calib.)

Tedesco, K. A., and R. Thunell (2003), Seasonal and interannual variations in planktonic foraminiferal flux and assemblage composition in the Cariaco Basin, Venezuela, *J. Foraminiferal Res.*, *33*(3), 192–210.

Tyrrell, T., and R. E. Zeebe (2004), History of carbonate ion concentration over the last 100 million years, *Geochim. Cosmochim. Acta*, *68*(17), 3521–3530.

Walter, L. M., and J. W. Morse (1985), The dissolution kinetics of shallow marine carbonates in seawater: A laboratory study, *Geochim. Cosmochim. Acta*, *49*, 1503–1514.

Watanabe, T., A. Winter, and T. Oba (2001), Seasonal changes in sea surface temperature and salinity during the Little Ice Age in the Caribbean Sea deduced from Mg/Ca and ^{18}O/^{16}O ratios in corals, *Mar. Geol.*, *173*, 21–35.

Watkins, J. M., and A. C. Mix (1998), Testing the effects of tropical temperature, productivity, and mixed-layer depth on foraminiferal transfer functions, *Paleoceanography*, *13*(1), 96–105.

Whitko, A. N., D. W. Hastings, and B. P. Flower (2002), Past sea surface temperatures in the tropical South China Sea based on a new foraminiferal Mg calibration, *MARsci*, doi:MARSci.2002.01.020101.

Williams, D. F., A. W. H. Bé, and R. G. Fairbanks (1981), Seasonal stable isotopic variations in living planktonic foraminifera from Bermuda plankton tows, *Palaeogeogr. Palaeoclimatol. Palaeoecol.*, *33*, 71–102.

Wüst, G. (1963), On the stratification and the circulation in the cold water sphere of the Antillean-Caribbean basins, *Deep Sea Res. Oceanogr. Abstr.*, *10*, 165–187.

Wüst, G. (Ed.) (1964), *Stratification and Circulation in the Antillean-Caribbean Basins, Part 1: Spreading and Mixing of the Water Types with an Oceanographic Atlas*, 201 pp., Columbia Univ. Press, New York.

Zahn, R., D. Meischner, and C. Hemleben (Eds.) (1996), *Research Vessel METEOR Cruise No. 35 (1996): Caribbean Sea, Sargasso Sea*, Inst. für Meereskunde der Univ. Hamburg, Leitstelle METEOR, Hamburg, Germany.